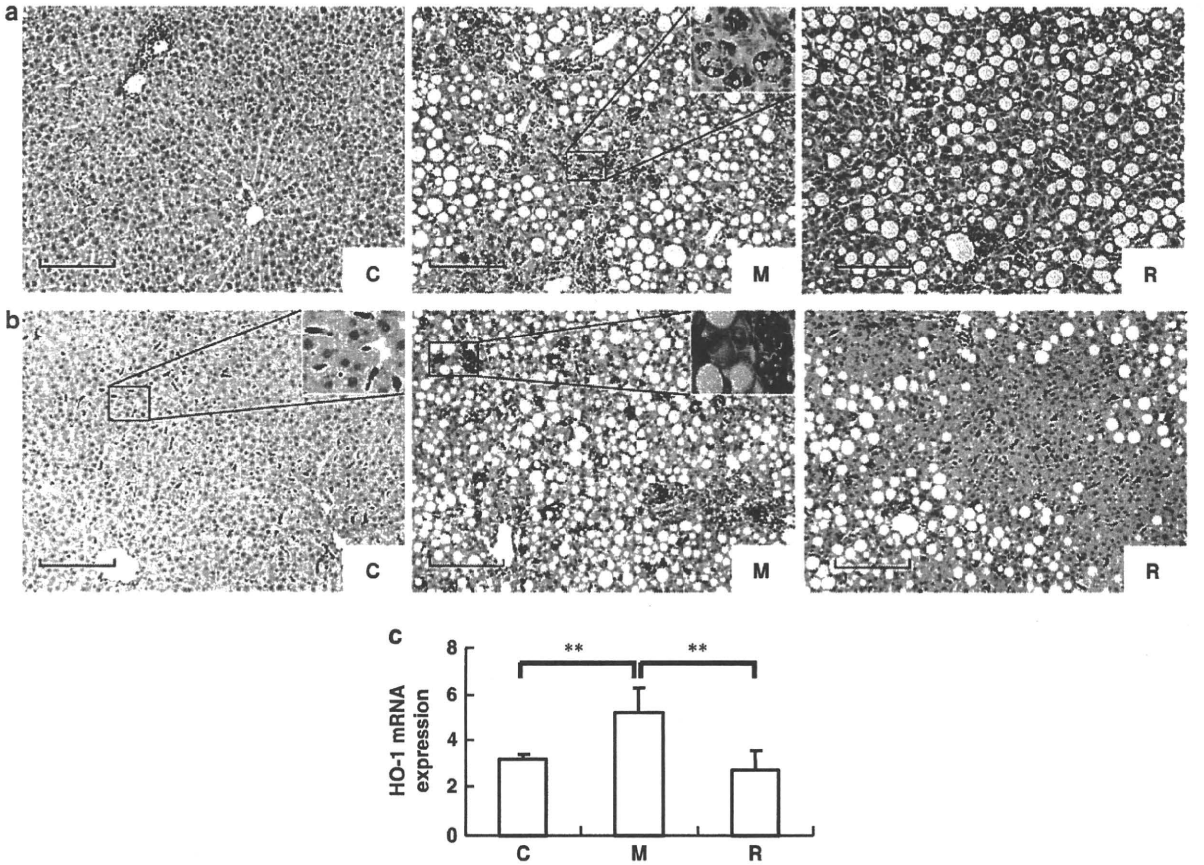

Figure 3 Immunohistochemistry of 4-HNE and HO-1, and the expression of HO-1 mRNA. (**a**) Immunohistochemistry of 4-HNE (× 200). Bar, 25 μm. There is a magnified view of the squared area (× 1000). Foamed macrophages are evident. (**b**) Immunohistochemistry of HO-1 (× 200). The box shows a higher magnification of the squared area. Bar, 25 μm. (**c**) HO-1 mRNA level. $^{**}P<0.01$. The HO-1 mRNA level was normalized by the GAPDH mRNA level.

Conversely, the *in situ* BrdU incorporation assay showed that the number of proliferated hepatocytes underwent no marked changes in group M compared with group C (7.5 ± 3 *vs* 7.6 ± 1.0 cells per field, respectively, $P>0.05$), whereas it increased significantly in group R (17.2 ± 4.35 cells per field) (Figure 5b and d). Furthermore, the ratio of hepatocyte proliferation (BrdU-positive cells)/apoptosis (TUNEL-positive cells) decreased significantly in group M compared with control group C (0.10 ± 0.03 *vs* 0.19 ± 0.03, respectively, $P<0.01$), whereas it increased significantly in group R compared with group M (0.41 ± 0.09, $P<0.01$, Figure 5e). In addition, as shown in Figure 5f, mRNA expression of IL-6, which is known to initiate hepatocyte growth through the STAT3 transcription factor, markedly decreased in group M and thereafter increased in group R, whereas STAT-3 expression remained unchanged (data not shown). Furthermore, mRNA expression of BAX and BAK, proapoptotic genes, markedly increased in group M and returned to the normal range in group R, whereas Bcl-xl and Bcl-2 mRNA expression remained unchanged (data not shown). These results suggest that hepatocyte proliferation/apoptosis undergoes a dynamic transition on changing the diet from MCDD to CD.

Involvement of ER Stress in Fibrosis of Steatohepatitis and its Recovery

Caspase-12 is known as a member of the IL-1β-converting enzyme subfamily of caspases. In rodents, the homolog of this gene mediates apoptosis in response to ER stress. Immunohistochemistry using anti-caspase-12 antibodies revealed that caspase-12 showed negligible expression in group C, whereas it was abundant in hepatocytes with fatty degeneration in group M, indicating the occurrence of ER stress in fatty hepatocytes (Figure 6a). The dietary change clearly reduced the content of caspase-12 in hepatocytes (Figure 6a).

Immunoblot analyses of ER stress-marker proteins such as caspase-12, caspase-7 and cleaved caspase-7, and GRP78 showed that all of these protein expressions were significantly increased in group M and successively reduced in group R (Figure 6b and c). In addition, PDI, an ER-residing protein that catalyzes protein folding and thiol-disulfide interchange reactions,[30,31] was markedly induced in group M compared with groups C and R (Figure 6d).

RT-PCR analyses supported these observations by showing that mRNAs of GRP78, caspase-12, caspase-7, c-Jun, and

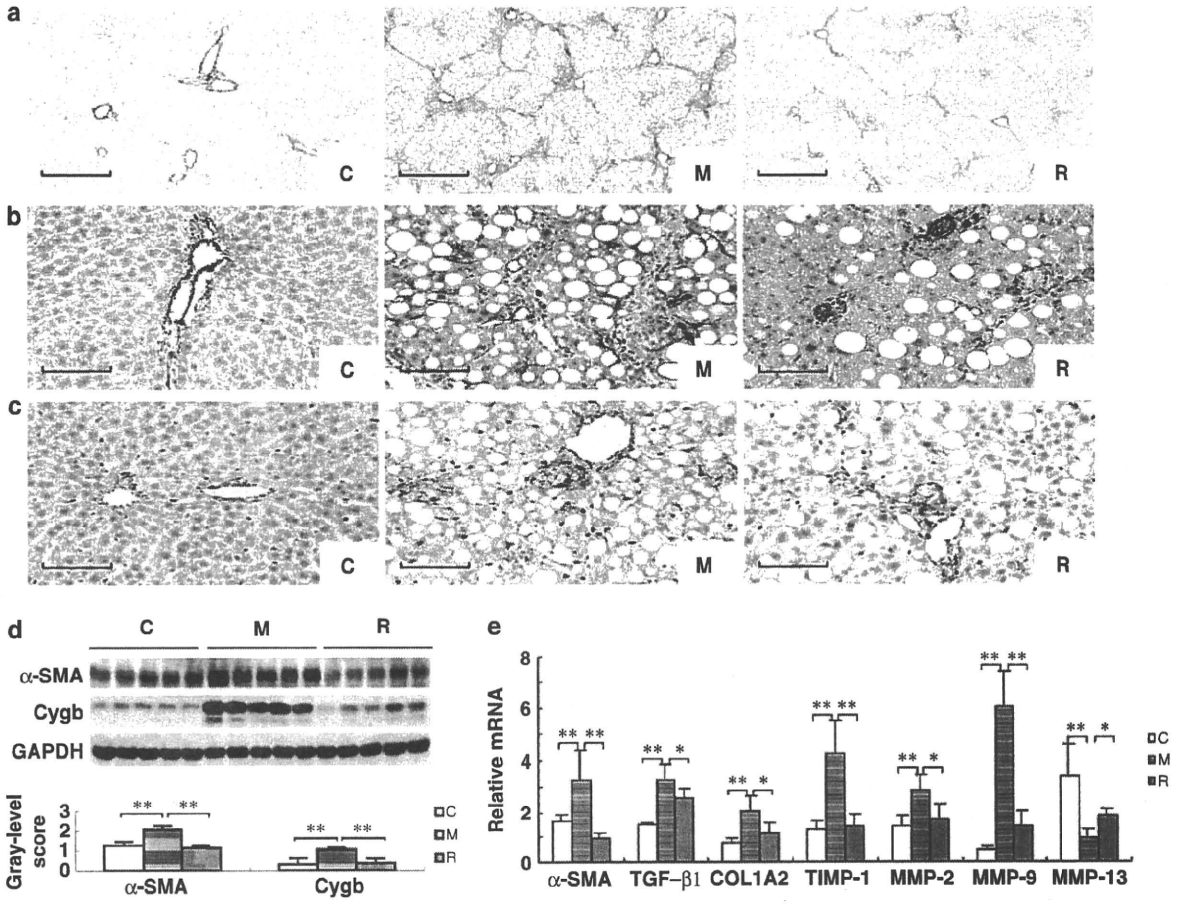

Figure 4 Hepatic stellate cell activation and liver fibrosis. (**a**) Sirius Red staining (× 100). Bar, 50 μm. (**b**) α-SMA immunostaining (× 400). α-SMA-positivity was seen only around large vessels in group C. In group M, α-SMA-positive cells colocalized in and around granulomas close to fatty hepatocytes and perisinusoidal spaces, indicating they were activated stellate cells. The number of α-SMA-positive cells was clearly reduced in group R. Bar, 12.5 μm. (**c**) Cygb immunostaining (× 400). Cygb-positivity was seen only along sinusoids in group C. In group M, Cygb-positive cells colocalized in and around granulomas close to fatty hepatocytes and perisinusoidal spaces, indicating that they were activated stellate cells. The number of Cygb-positive cells was clearly reduced in group R. Bar, 12.5 μm. (**d**) Immunoblotting for α-SMA and Cygb. The gray-level score indicates the histogram of immunoblotting for α-SMA and Cygb. $^{**}P<0.01$. (**e**) Fibrotic gene expressions in the liver determined by qRT-PCR. Relative mRNA levels of α-SMA, TGFβ1, Col1A2, TIMP-1, MMP-2, MMP-9, and MMP-13. mRNA levels were normalized by GAPDH. $^{*}P<0.05$, $^{**}P<0.01$.

ERp57 increased significantly in group C and decreased after 2 weeks of CD diet administration (Figure 6e).

DISCUSSION

Hepatic Steatosis: the 'Primer' for Fibrosis of NASH Induced by MCDD

As both methionine and choline are essential precursors of hepatic phosphatidylcholine synthesis, their deficiency provokes hepatic steatosis by limiting the availability of its substrates, which, in turn, inhibits VLDL assembly and blocks TG secretion from hepatocytes.[32,33] Our study showed that serum levels of TG and FFA in MCDD-induced fatty liver fibrosis (group M) decreased to one-fifth and two-thirds, respectively, of that in the CD group (group C), indicating the impaired secretion of TG and FFA from hepatocytes. Hepatic steatosis facilitates the mitochondrial uptake of FFA, the overflow of which triggers β-oxidation, resulting in the generation of reactive oxygen radicals to trigger lipid peroxidation.[34,35] This leads to the production of toxic substances that damage the mitochondria and stimulate further production of reactive oxygen species.[34] Such a positive feedback loop results in cellular damage, activation of liver macrophages (Kupffer cells), and generation of proinflammatory cytokines that initiate hepatic inflammation.[36,37]

Kupffer cells could be the main source of TNF-α in MCDD-induced liver injury. In addition, MMP-9 (gelatinase B), a member of MMPs, is derived mainly from Kupffer cells in the liver,[38] and its expression is significantly increased together with the activation of cells, indicating that MMP-9 could be a marker of Kupffer cell activation instead of its activity as a collagenase. A number of studies have shown increased serum and plasma levels of MMP-9 in various types

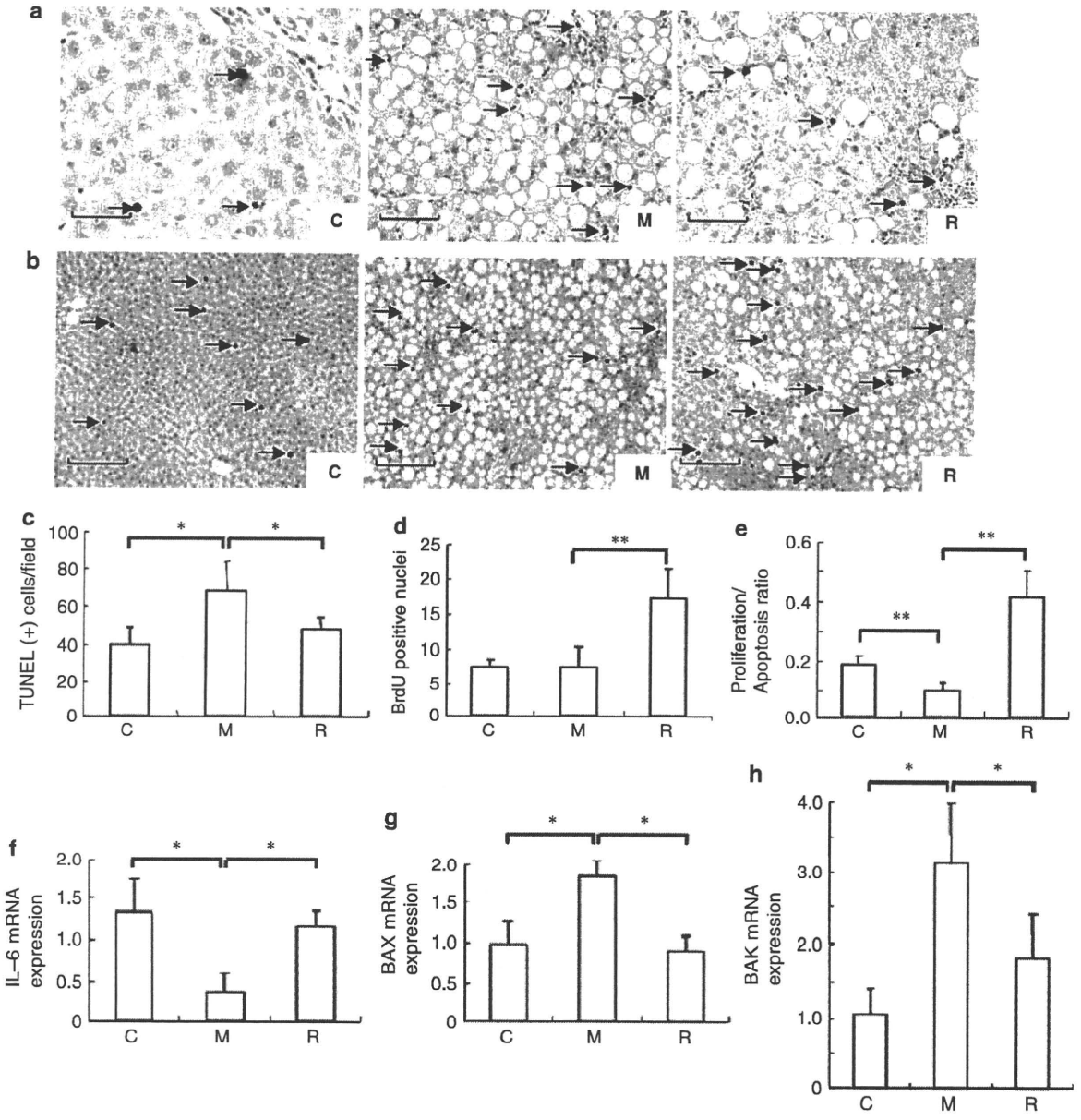

Figure 5 Changes in hepatocyte apoptosis and proliferation. (**a**) A typical photograph of apoptotic hepatocytes (TUNEL staining, arrows) (× 400). TUNEL-positive cells were counted under a microscope in > 100 unselected 20 × microscopic fields per liver. Bar, 12.5 μm. (**b**) A typical photograph of proliferating hepatocytes (BrdU staining, arrows) (× 200). Bar, 25 μm. (**c**) Bar graphs indicate the number of TUNEL-positive cells per field. $^{*}P<0.05$. (**d**) Bar graphs indicate the number of BrdU-positive cells per field. $^{**}P<0.01$. (**e**) The ratio of proliferation/apoptosis of hepatocytes. $^{*}P<0.05$. $^{**}P<0.01$. (**f–h**) Levels of IL-6, BAX, and BAK mRNA. The IL-6, BAX, and BAK mRNA levels determined by RT-PCR. The mRNA level was normalized by the GAPDH mRNA level. $^{**}P<0.01$.

of liver injury, including ischemic reperfusion injury[39] and chronic viral hepatitis.[40,41] Furthermore, the mutation of MMP-9 was reported to inhibit hepatic fibrogenesis in mice.[42] This study showed that MMP-9 and TNF-α mRNA expression increased significantly with the activation of Kupffer cells that were positive for CD68 in group M, whereas switching the diet from MCDD to CD triggered the immediate recovery of MMP-9, suggesting that MMP-9 is associated with the activation status of Kupffer cells.

In contrast, Kupffer cells have been reported to have an important role in the regression of fibrosis through the expression of MMP-13 in other experimental models.[43,44] The current study showed that the number of CD68- and HO-1-positive cells, which are identical to activated Kupffer cells, significantly increased in group M, whereas MMP-13 mRNA expression markedly decreased. Switching the diet from MCDD to CD triggered the immediate recovery of the liver histology, accompanied by a marked increase in the expression

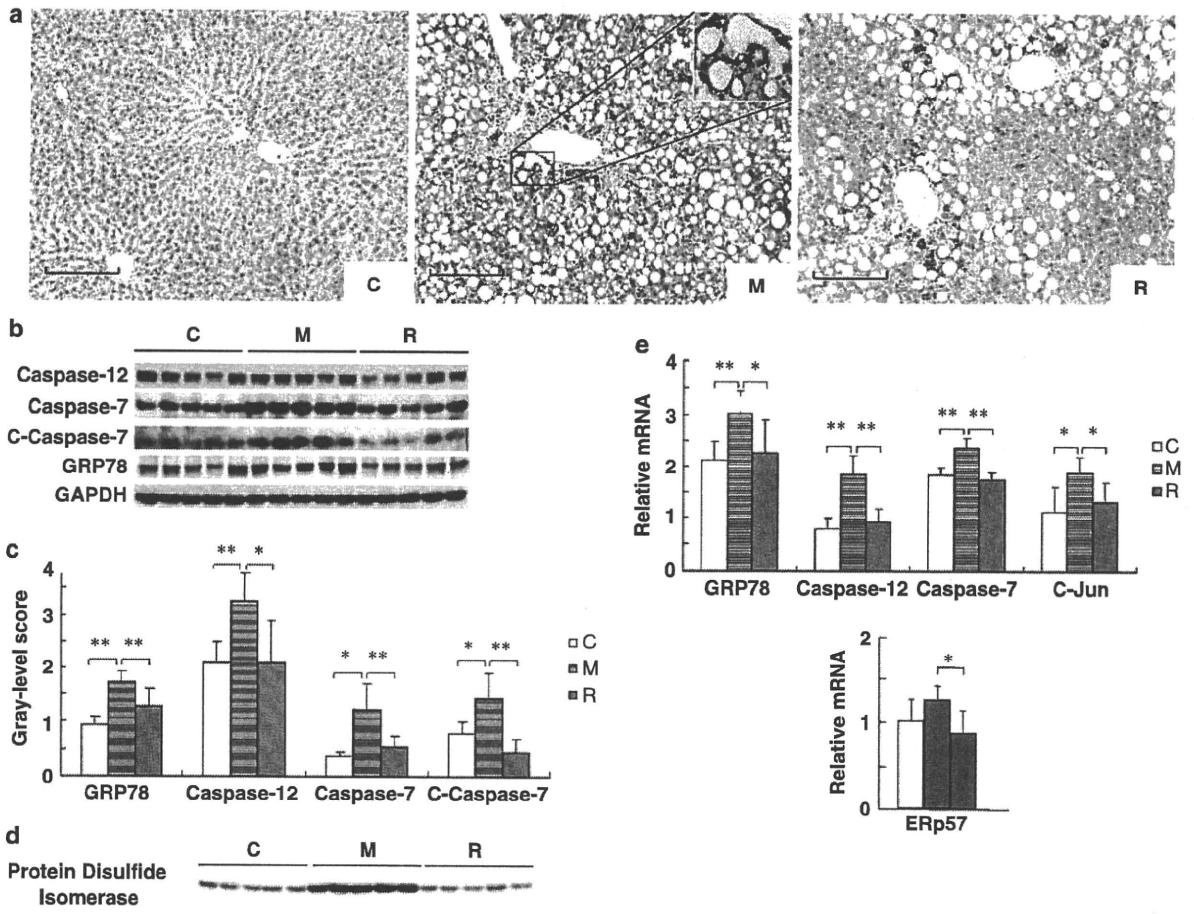

Figure 6 Endoplasmic reticulum stress. (**a**) Caspase-12 immunostaining. Caspase-12-positive cells were rare in group C, whereas hepatocytes with fatty degeneration exhibited caspase-12 positivity in group M. In group R, caspase-12 was retained in hepatocytes with fat, whereas it disappeared in intact hepatocytes. Bar, 25 μm. The box shows an enlarged view of caspase-12-positive hepatocytes with fatty degeneration. (**b**) Immunoblotting of caspase-12, caspase-7, cleaved caspase-7, and GRP78. (**c**) The gray-level score determined by densitometry of the bands on immunoblotting for GRP78, caspase-12, caspase-7, and cleaved caspase-7. (**d**) Immunoblotting of protein disulfide isomerase. (**e**) Relative mRNA levels of GRP78, caspase-12, caspase-7, c-Jun, and ERp57 in groups C, M, and R. mRNA levels were normalized by GAPDH. $^{*}P<0.05$, $^{**}P<0.01$.

of MMP-13 mRNA, indicating the active role of MMP-13 derived from Kupffer cells in the regression of liver fibrosis.[45]

Stellate Cell Activation: a Crucial Role in Fibrosis Development in NASH

Hepatic stellate cells are present in the normal liver in a quiescent state, and their major function seems to be the storage of vitamin A. After injury, stellate cells activate or trans-differentiate into proliferating myofibroblast-like cells that produce abundant levels of fibrillar collagen and TIMP-1.[46] The secretion of abundant levels of TIMP-1 by activated stellate cells inhibits hepatic collagenase activity, and thereby promotes a net increase in extracellular matrix materials. TIMP-1 also promotes hepatic fibrogenesis by inhibiting the apoptosis of activated stellate cells.[47] MMP-2 (gelatinase A), derived mainly from activated stellate cells, is involved in degradation of the basement membrane in the early stage of liver fibrosis.[48] This study showed that both hepatic collagen deposition and stellate cell activation markers, such as α-SMA and cytoglobin, increased significantly with a markedly elevated expression of Col1A2, TIMP-1, MMP-2, and TGFβ-1 mRNAs. After switching to CD feeding, hepatic collagen deposition decreased significantly, accompanied by the marked reduction of these mRNAs, suggesting that MCDD-induced fatty liver fibrosis was closely related to stellate cell activation.

ER Stress: an Important Participant in Advancement of Liver Fibrosis in NASH

Obesity is associated with the induction of ER stress predominantly in the liver and adipose tissues.[49] Previous research has shown that fatty liver induced by a high sucrose

diet and high saturated fat diet shows clear ER stress events in a rodent model.[50] In addition, CHOP (a key component in ER stress-mediated apoptosis) deficiency attenuates cholestasis-induced liver fibrosis by reducing hepatocyte injury in bile duct ligation mice.[51] However, the roles of ER stress in fatty liver induced by MCDD have not been reported. Initial mediators of ER stress responses are ER resident type I transmembrane serine/threonine protein kinases, PKR-like ER kinase, and inositol-requiring enzyme-1(IRE-1); the accumulation of unfolded proteins in ER induces the oligomerization-dependent autophosphorylation of these kinases,[52,53] and thereby initiates cytoplasmic signal transduction. It was recently shown that activated IRE-1 on the ER membrane recruits TNF receptor-associated factor 2, and thus activates c-Jun amino-terminal kinase.[54] In addition, the survival response activates genes that encode ER-residing chaperones such as GRP78/Bip, which uses energy derived from ATP hydrolysis to prevent the aggregation of ER proteins and is considered the classical marker of UPR activation.[55] The current study showed that the expression of ER stress markers GRP78 (protein and mRNA) and c-Jun mRNA increased significantly in the MCDD group, whereas the expression of all of them decreased markedly after changing the diet. Another ER stress-related molecule, PDI,[30,31] showed similar behavior (Figure 6d and e). Thus, ER stress may be a key factor in MCDD-induced fatty liver fibrosis.

Caspases also participate in ER stress-induced apoptosis. In mice, procaspase-12 is localized on the cytoplasmic side of the ER and is cleaved and activated specifically by ER stress, but not by death receptor or mitochondria-mediated apoptotic signals.[56] Caspase-7, which translocates from the cytosol to the cytoplasmic side of the ER membrane in response to ER stress, has been reported to interact with and cleave procaspase-12, leading to its activation.[57] Activated caspase-12 then cleaves and activates procaspase-9, which in turn activates the downstream caspase cascade, including caspase-3, DNA fragmentation, and cell death.[58] Our results also showed that protein and gene expressions of caspase-12, caspase-7, and cleaved caspase-7 were significantly elevated during steatohepatitis together with the increased number of apoptotic hepatocytes, whereas they were reduced markedly after changing the diet. Furthermore, although the proliferation of hepatocytes did not show a clear change in the MCDD group, the ratio of hepatocyte proliferation/apoptosis decreased significantly, whereas it increased markedly after changing the diet to CD, indicating that the apoptotic caspase-12 pathway may also inhibit hepatocyte proliferation in MCDD-induced steatohepatitis. The marked elevation of BAX and BAK may also participate in stimulating the apoptosis of hepatocytes by MCDD.

In conclusion, this study shows that, although the underlying mechanisms involved in MCDD-induced fatty liver fibrosis are complicated, they may include not only well-known factors, such as steatosis, oxidative stress, and the activation of Kupffer and stellate cells, but also ER stresses and the balance between hepatocyte proliferation and apoptosis. The reversibility of liver fibrosis is also shown in steatohepatitis, at least in the present MCDD model.

Supplementary Information accompanies the paper on the Laboratory Investigation website (http://www.laboratoryinvestigation.org)

ACKNOWLEDGEMENTS

NK was supported by a Grant-in-Aid for Scientific Research from the Japan Society for the Promotion of Science through Grant no. 18659214 (2007), by a Grant for Research on Hepatitis from the Ministry of Health, Labour and Welfare (2008), and by a Trust Area Research Grant from Osaka City University (2008). We thank Dr Ryoko Shiga for her valuable discussion about this paper.

DISCLOSURE/CONFLICT OF INTEREST

The authors declare no conflict of interest.

1. Angulo P. Nonalcoholic fatty liver disease. N Engl J Med 2002; 346:1221–1231.
2. Clark JM, Diehl AM. Hepatic steatosis and type 2 diabetes mellitus. Curr Diab Rep 2002;2:210–215.
3. Festi D, Colecchia A, Sacco T, *et al.* Hepatic steatosis in obese patients: clinical aspects and prognostic significance. Obes Rev 2004;5:27–42.
4. Bedogni G, Miglioli L, Masutti F, *et al.* Prevalence of and risk factors for nonalcoholic fatty liver disease: the Dionysos nutrition and liver study. Hepatology 2005;42:44–52.
5. Boccato S, Pistis R, Noventa F, *et al.* Fibrosis progression in initially mild chronic hepatitis C. J Viral Hepat 2006;13:297–302.
6. Fartoux L, Chazouillères O, Wendum D, *et al.* Impact of steatosis on progression of fibrosis in patients with mild hepatitis C. Hepatology 2005;41:82–87.
7. Leandro G, Mangia A, Hui J, *et al.* Relationship between steatosis, inflammation and fibrosis in chronic hepatitis C: a meta-analysis of individual patient data. Gastroenterology 2006;130:1636–1642.
8. Sass DA, Chang P, Chopra KB. Nonalcoholic fatty liver disease: a clinical review. Dig Dis Sci 2005;50:171–180.
9. Bugianesi E, Leone N, Vanni E, *et al.* Expanding the natural history of nonalcoholic steatohepatitis: from cryptogenic cirrhosis to hepatocellular carcinoma. Gastroenterology 2002;123:134–140.
10. Shimada M, Hashimoto E, Taniai M, *et al.* Hepatocellular carcinoma in patients with non-alcoholic steatohepatitis. J Hepatol 2002;37: 154–160.
11. Bugianesi E. Review article: steatosis, the metabolic syndrome and cancer. Aliment Pharmacol Ther 2005;22(Suppl 2):40–43.
12. Kelley DE, McKolanis TM, Hegazi RA, *et al.* Fatty liver in type 2 diabetes mellitus: relation to regional adiposity, fatty acids, and insulin resistance. Am J Physiol Endocrinol Metab 2003;285:E906–E916.
13. Shiratori Y, Imazeki F, Moriyama M, *et al.* Histologic improvement of fibrosis in patients with hepatitis C who have sustained response to interferon therapy. Ann Intern Med 2000;132:517–524.
14. Poynard T, McHutchison J, Davis GL, *et al.* Impact of interferon alfa-2b and ribavirin on progression of liver fibrosis in patients with chronic hepatitis C. Hepatology 2000;32:1131–1137.
15. Yuan M, Konstantopoulos N, Lee J, *et al.* Reversal of obesity- and diet-induced insulin resistance with salicylates or targeted disruption of Ikkbeta. Science 2001;293:1673–1677.
16. Uysal KT, Wiesbrock SM, Marino MW, *et al.* Protection from obesity-induced insulin resistance in mice lacking TNF-alpha function. Nature 1997;389:610–614.
17. Hirosumi J, Tuncman G, Chang L, *et al.* A central role for JNK in obesity and insulin resistance. Nature 2002;420:333–336.
18. Hampton RY. ER stress response: getting the UPR hand on misfolded proteins. Curr Biol 2000;10:R518–R521.
19. Mori K. Tripartite management of unfolded proteins in the endoplasmic reticulum. Cell 2000;101:451–454.
20. Harding HP, Calfon M, Urano F, *et al.* Transcriptional and translational control in the mammalian unfolded protein response. Annu Rev Cell Dev Biol 2002;18:575–599.

21. Ji C, Kaplowitz N. Betaine decreases hyperhomocysteinemia, endoplasmic reticulum stress, and liver injury in alcohol-fed mice. Gastroenterology 2003;124:1488–1499.
22. Rodrigues CM, Ma X, Linehan-Stieers C, *et al.* Ursodeoxycholic acid prevents cytochrome c release in apoptosis by inhibiting mitochondrial membrane depolarization and channel formation. Cell Death Differ 1999;6:842–854.
23. Pavio N, Romano PR, Graczyk TM, *et al.* Protein synthesis and endoplasmic reticulum stress can be modulated by the hepatitis C virus envelope protein E2 through the eukaryotic initiation factor 2 alpha kinase PERK. J Virol 2003;77:3578–3585.
24. Tardif KD, Mori K, Siddiqui A. Hepatitis C virus subgenomic replicons induce endoplasmic reticulum stress activating an intracellular signaling pathway. J Virol 2002;76:7453–7459.
25. Kawada N, Kristensen DB, Asahina K, *et al.* Characterization of a stellate cell activation-associated protein (STAP) with peroxidase activity found in rat hepatic stellate cells. J Biol Chem 2001;276:25318–25323.
26. Nakatani K, Seki S, Kawada N, *et al.* Expression of SPARC by activated hepatic stellate cells and its correlation with the stages of fibrogenesis in human chronic hepatitis. Virchows Arch 2002;441:466–474.
27. Otogawa K, Kinoshita K, Fujii H, *et al.* Erythrophagocytosis by liver macrophages (Kupffer cells) promotes oxidative stress, inflammation, and fibrosis in a rabbit model of steatohepatitis: implications for the pathogenesis of human nonalcoholic steatohepatitis. Am J Pathol 2007;170:967–980.
28. Wang YQ, Ikeda K, Ikebe T, *et al.* Inhibition of hepatic stellate cell proliferation and activation by the semisynthetic analogue of fumagillin TNP-470 in rats. Hepatology 2000;32:980–989.
29. Uyama N, Shimahara Y, Okuyama H, *et al.* Carbenoxolone inhibits DNA synthesis and collagen gene expression in rat hepatic stellate cells in culture. J Hepatol 2003;39:749–755.
30. Riemer J, Bulleid N, Herrmann JM. Disulfide formation in the ER and mitochondria: two solutions to a common process. Science 2009;324:1284–1287.
31. Nakamura T, Lipton SA. Cell death: protein misfolding and neurodegenerative diseases. Apoptosis 2009;14:455–468.
32. Vance JE, Vance DE. The role of phosphatidylcholine biosynthesis in the secretion of lipoproteins from hepatocytes. Can J Biochem Cell Biol 1985;63:870–881.
33. Yao ZM, Vance DE. The active synthesis of phosphatidylcholine is required for very low density lipoprotein secretion from rat hepatocytes. J Biol Chem 1988;263:2998–3004.
34. Fromenty B, Robin MA, Igoudjil A, *et al.* The ins and outs of mitochondrial dysfunction in NASH. Diabetes Metab 2004;30:121–138.
35. Pessayre D, Fromenty B. NASH: a mitochondrial disease. J Hepatol 2005;42:928–940.
36. Albano E, Mottaran E, Occhino G, *et al.* Review article: role of oxidative stress in the progression of non-alcoholic steatosis. Aliment Pharmacol Ther 2005;22:71–73.
37. Day CP. From fat to inflammation. Gastroenterology 2006;130:207–210.
38. Winwood PJ, Schuppan D, Iredale JP, *et al.* Kupffer cell-derived 95 kDa type IV collagenase/gelatinase B: characterisation and expression in cultured cells. Hepatology 1995;22:304–315.
39. Kuyvenhoven JP, Verspaget HW, Gao Q, *et al.* Assessment of serum matrix metalloproteinases MMP-2 and MMP-9 after human liver transplantation: increased serum MMP-9 level in acute rejection. Transplantation 2004;77:1646–1652.
40. Leroy V, Monier F, Bottari S, *et al.* Circulating matrix metalloproteinases 1, 2, 9 and their inhibitors TIMP-1 and TIMP-2 as serum markers of liver fibrosis in patients with chronic hepatitis C: comparison with PIIINP and hyaluronic acid. Am J Gastroenterol 2004;799:271–279.
41. Chung TW, Kim JR, Suh JI, *et al.* Correlation between plasma levels of matrix metalloproteinase (MMP)-9/MMP-2 ratio and alpha-fetoproteins in chronic hepatitis carrying hepatitis B virus. J Gastroenterol Hepatol 2004;19:565–571.
42. Roderfeld M, Weiskirchen R, Wagner S, *et al.* Inhibition of hepatic fibrogenesis by matrix metalloproteinase-9 mutants in mice. FASEB J 2006;20:444–454.
43. Hironaka K, Sakaida I, Matsumura Y, *et al.* Enhanced interstitial collagenase (matrix metalloproteinase-13) production of Kupffer cell by gadolinium chloride prevents pig serum-induced rat liver fibrosis. Biochem Biophys Res Commun 2000;267:290–295.
44. Sakaida I, Hironaka K, Terai S, *et al.* Gadolinium chloride reverses dimethylnitrosamine (DMN)-induced rat liver fibrosis with increased matrix metalloproteinases (MMPs) of Kupffer cells. Life Sci 2003;72:943–959.
45. Friedman S. Mac the knife? Macrophages —the double-edged sword of hepatic fibrosis. J Clin Invest 2005;115:29–32.
46. Iredale JP, Benyon RC, Arthur MJ, *et al.* Tissue inhibitor of metalloproteinase-1 messenger RNA expression is enhanced relative to interstitial collagenase messenger RNA in experimental liver injury and fibrosis. Hepatology 1996;24:176–184.
47. Iredale JP, Murphy G, Hembry RM, *et al.* Human hepatic lipocytes synthesize tissue inhibitor of metalloproteinases-1. Implications for regulation of matrix degradation in liver. J Clin Invest 1992;90:282–287.
48. Winwood PJ, Schuppan D, Iredale JP, *et al.* Kupffer cell-derived 95-kd type IV collagenase/gelatinase B: characterization and expression in cultured cells. Hepatology 1995;22:304–315.
49. Ozcan U, Cao Q, Yilmaz E, *et al.* Hotamisligil. Endoplasmic reticulum stress links obesity, insulin action, and type 2 diabetes. Science 2004;306:457–461.
50. Wang D, Wei Y, Pagliassotti MJ. Saturated fatty acids promote endoplasmic reticulum stress and liver injury in rats with hepatic steatosis. Endocrinology 2006;147:943–951.
51. Tamaki N, Hatano E, Taura K, *et al.* CHOP deficiency attenuates cholestasis-induced liver fibrosis by reduction of hepatocyte injury. Am J Physiol Gastrointest Liver Physiol 2008;294:G498–G505.
52. Bertolotti A, Zhang Y, Hendershot LM, *et al.* Dynamic interaction of BiP and ER stress transducers in the unfolded-protein response. Nat Cell Biol 2000;2:326–332.
53. Liu CY, Schröder M, Kaufman RJ. Ligand-independent dimerization activates the stress response kinases IRE1 and PERK in the lumen of the endoplasmic reticulum. J Biol Chem 2000;275:24881–24885.
54. Urano F, Wang X, Bertolotti A, *et al.* Coupling of stress in the ER to activation of JNK protein kinases by transmembrane protein kinase IRE1. Science 2000;287:664–666.
55. Iwawaki T, Hosoda A, Okuda T, *et al.* Translational control by the ER transmembrane kinase/ribonuclease IRE1 under ER stress. Nat Cell Biol 2001;3:158–164.
56. Nakagawa T, Yuan J. Cross-talk between two cysteine protease families. Activation of caspase-12 by calpain in apoptosis. J Cell Biol 2000;150:887–894.
57. Rao RV, Hermel E, Castro-Obregon S, *et al.* Coupling endoplasmic reticulum stress to the cell death program: mechanism of caspase activation. J Biol Chem 2001;276:33869–33874.
58. Tan Y, Dourdin N, Wu C, *et al.* Ubiquitous calpains promote caspase-12 and JNK activation during endoplasmic reticulum stress-induced apoptosis. J Biol Chem 2006;281:16016–16024.

Biochemical and Biophysical Research Communications 391 (2010) 316–321

Contents lists available at ScienceDirect

Biochemical and Biophysical Research Communications

journal homepage: www.elsevier.com/locate/ybbrc

Suppression of type I collagen production by microRNA-29b in cultured human stellate cells

Tomohiro Ogawa [a], Masashi Iizuka [a], Yumiko Sekiya [a,b], Katsutoshi Yoshizato [a,c], Kazuo Ikeda [d], Norifumi Kawada [a,*]

[a] Department of Hepatology, Graduate School of Medicine, Osaka City University, Osaka, Japan
[b] Toray Industries Inc., Kanagawa, Japan
[c] PhoenixBio Co. Ltd., Hiroshima, Japan
[d] Department of Functional Anatomy, Graduate School of Medicine, Nagoya City University, Aichi, Japan

ARTICLE INFO

Article history:
Received 6 November 2009
Available online 12 November 2009

Keywords:
Liver fibrosis
SP1
TGF-β
Interferon
TargetScan

ABSTRACT

MicroRNAs (miRNAs) are small noncoding RNAs that regulate gene expression through imperfect base pairing with the 3′ untranslated region (3′UTR) of target mRNA. We studied the regulation of alpha 1 (I) collagen (Col1A1) expression by miRNAs in human stellate cells, which are involved in liver fibrogenesis. Among miR-29b, -143, and -218, whose expressions were altered in response to transforming growth factor-β1 or interferon-α stimulation, miR-29b was the most effective suppressor of type I collagen at the mRNA and protein level via its direct binding to Col1A1 3′UTR. miR-29b also had an effect on SP1 expression. These results suggested that miR-29b is involved in the regulation of type I collagen expression by interferon-α in hepatic stellate cells. It is anticipated that miR-29b will be used for the regulation of stellate cell activation and lead to antifibrotic therapy.

Introduction

Hepatic stellate cells, which reside in the Disse's space outside the liver sinusoids, maintain a quiescent phenotype and store vitamin A under physiological conditions [1,2]. When liver injury occurs due to alcohol abuse, hepatitis viral infection, or obesity, stellate cells activate in response to inflammatory stimuli and become myofibroblastic cells that express smooth muscle α-actin as a representative marker [2]. Myofibroblastic cells secrete profibrogenic mediators, such as transforming growth factor-β (TGF-β), connective tissue growth factor, and tissue inhibitor of matrix metalloproteinases, and generate extracellular matrix materials including collagens, fibronectin, and laminin; thus, they play a pivotal role in liver fibrogenesis [3]. In particular, collagen production by activated stellate cells is regulated by TGF-β in an autocrine loop, which is accompanied by the induction of TGF-β receptors [4]. Suppression of hepatic stellate cell activation and collagen expression is thus a critical issue to establish therapeutic strategies for human liver fibrosis [1,5].

MicroRNAs (miRNAs) are endogenous small noncoding RNAs that modulate gene expression through imperfect base pairing with the 3′ untranslated region (UTR) of target mRNA, resulting in the inhibition of translation or the promotion of mRNA degradation [6,7]. miRNAs play roles in cell proliferation [8], development [9], and differentiation [10], and their contribution to human diseases such as cancer, cardiomyopathies, and schizophrenia have been reported [11–13]. miR-122 is also involved in the defense system against viral hepatitis C with regard to interferon (IFN)-β therapy [14], and miR-26 expression status is associated with survival and response to adjuvant IFNα therapy in patients with hepatocellular carcinoma [15]. Some miRNAs are involved in liver development and hepatocyte lipid metabolism [16–18].

Recent studies have shown that miRNAs are additionally involved in the alteration of hepatic stellate cell phenotypes; down-regulation of miR-27a and -27b allows culture-activated rat stellate cells to return to a quiescent phenotype with abundant vitamin A storage and decreased cell proliferation [19]; miR-15b and -16, which target the Bcl-2 and caspase signaling pathways, may affect stellate cell activation and liver fibrosis [20]. However, the function of miRNAs in hepatic stellate cell activation and their collagen production is largely unknown.

Here, we show that miR-29b, which is induced in human stellate cells (LX-2) treated with IFNα, is a potential regulator of type I collagen mRNA and protein expression. Although the primary action of IFNs is to eradicate viruses, i.e., hepatitis B and C viruses in

Abbreviations: Col1A1, alpha 1 (I) collagen; DMEM, Dulbecco's modified Eagle's medium; FBS, fetal bovine serum; IFN, interferon; miRNAs, microRNAs; TGF-β, transforming growth factor-β; UTR, untranslated region.

* Corresponding author. Address: Department of Hepatology, Graduate School of Medicine, Osaka City University, 1-4-3, Asahimachi, Abeno, Osaka 545-8585, Japan. Fax: +81 6 6646 9072.
E-mail address: kawadanori@med.osaka-cu.ac.jp (N. Kawada).

0006-291X/$ - see front matter © 2009 Elsevier Inc. All rights reserved.
doi:10.1016/j.bbrc.2009.11.056

the case of the liver, IFNs also exhibit an antifibrotic action in human chronic hepatitis [21,22] and rodent liver fibrosis models [23]. Our data suggest that miR-29b may be a novel regulator of type I collagen expression in addition to its involvement in the well-known Smad cascade. Moreover, miR-29b upregulation may play a partial role in the antifibrotic action of IFNs.

Materials and methods

Materials. Recombinant human TGF-β1 was purchased from PeproTech (London, UK). Human natural IFNα was obtained from Otsuka Pharmaceutical Co. (Tokushima, Japan). Precursors of miR-29b, -143, and -218, and the negative control were purchased from Ambion (Austin, TX, USA). Dulbecco's modified Eagle's medium (DMEM) and fetal bovine serum (FBS) were purchased from Sigma Chemical Co. (St. Louis, MO, USA). Rabbit monoclonal antibodies against Smad2 and phospho-Smad2 were purchased from Cell Signaling Technology Inc. (Beverly, MA, USA). The mouse monoclonal antibody against SP1 was purchased from Bio Matrix Research Inc. (Chiba, Japan). Rabbit polyclonal antibody against type I collagen was purchased from Rockland Immunochemicals, Inc. (Gilbertsville, PA, USA). Mouse monoclonal antibody against GAPDH was purchased from Chemicon International Inc. (Temecula, CA, USA). Enhanced Chemiluminescence plus detection reagent was purchased from GE Healthcare (Buckinghamshire, UK). Immobilon P membranes were purchased from Millipore Corp. (Bedford, MA, USA). All other reagents were purchased from Sigma Chemical Co. or Wako Pure Chemical Co. (Osaka, Japan).

Preparation of the human hepatic stellate cell line LX-2. The human hepatic stellate cell line (LX-2, donated by Dr. Scott Friedman), which was spontaneously immortalized by growth in low serum, was established as reported previously [24]. Characterizations of the cells are described in detail elsewhere. The cells were maintained on plastic culture plates in DMEM supplemented with 10% FBS. After the culture had continued for the indicated number of days, the medium was replaced with DMEM supplemented with 0.1% FBS plus test agents, and the culture was continued for another 24 h.

Quantitative real-time PCR. Total RNA was extracted from human stellate cells using the miRNeasy Mini Kit (Qiagen, Valencia, CA, USA). cDNAs were synthesized using 0.5 μg of total RNA, ReverTra Ace (Toyobo, Osaka, Japan), and oligo(dT)$_{12-18}$ primers according to the manufacturer's instructions [25]. Gene expression was measured by real-time PCR using cDNA, real-time PCR Master Mix Reagents (Toyobo), and a set of gene-specific oligonucleotide primers (alpha 1 (I) collagen [Col1A1]: Forward 5′-CCCGGGTTTCAGAGACA ACTTC-3′, Reverse 5′-TCCACATGCTTTATTCCAGCAATC-3′; TGF-β1: Forward 5′-AGCGACTCGCCAGAGTGGTTA-3′, Reverse 5′-GCAGTG TGTTATCCCTGCTGTCA-3′; SP1: Forward 5′-TCGGATGAGCTACA GAGGCACAA-3′, Reverse 5′-GTCACTCCTCATGAAGCGCTTAGG-3′; and GAPDH: Forward 5′-GCACCGTCAAGGCTGAGAAC-3′, Reverse 5′-TGGTGAAGACGCCAGTGGA-3′) with an Applied Biosystems Prism 7500 (Applied Biosystems, Foster City, CA, USA). To detect miRNA expression, the RT reaction was performed using the TaqMan MicroRNA Assay (Applied Biosystems) according to the manufacturer's instructions. The GAPDH level was measured and used to normalize the relative abundance of mRNAs and miRNAs.

Immunoblot. Proteins (20–50 μg) were subjected to sodium dodecyl sulfate–polyacrylamide gel electrophoresis and then transferred onto Immobilon P membranes. After blocking, the membranes were treated with primary antibodies, followed by peroxidase-conjugated secondary antibodies. Immunoreactive bands were visualized by the enhanced chemiluminescence system using the Fujifilm Image Reader LAS-3000 (Fuji Medical Systems, Stamford, CT, USA).

Transient transfection of miRNA precursors. Precursors of miR-29b, -143, and -218, and the negative control were transfected into human stellate cells using Lipofectamine 2000 (Invitrogen, Carlsbad, CA, USA) at a final concentration of 50 nM. Briefly, the cells were plated in DMEM supplemented with 10% FBS at a density of 1–2 × 10^5 cells/ml 24 h prior to the transfection. miRNA precursors and Lipofectamine 2000 were mixed at a ratio of 25 (pmol):1 (μl) in Opti-MEM I Reduced Medium (Invitrogen) and incubated for 20–30 min at room temperature. The miRNA precursor–Lipofectamine 2000 complexes were then added to stellate cell culture medium. After 6 h, the culture medium was changed, and TGF-β1 was added at a concentration of 2 ng/ml.

Luciferase reporter assay. 3′UTRs containing putative miRNA target regions of the Col1A1 and SP1 genes were obtained by PCR using human stellate cell cDNA as a template and primer sets as follows: Col1A1–miR-29: Forward 5′-TTCTCGAGGTTCTTGTCTTG ATGTGTCACC-3′, Reverse 5′-TTTCTAGAGAGAGCAGAGGCCTGAGA AG-3′; Col1A1–miR-143: Forward 5′-CTCGAGACTCCCTCCATCCCAA CCT-3′, Reverse 5′-TCTAGAATTGCTGGGCAGACAATAC-3′; Col1A1–miR-218: Forward 5′-CTCGAGGTGGATGGGGACTTGTGAAT-3′, Reverse 5′-TCTAGATTATGTTTGGGTCATTTCCAC-3′; SP1–miR-29: Forward 5′-TTCTCGAGTGGGTGCTACACAGAATGC-3′, Reverse 5′-TTTC TAGAAGACTGTCCTTATTTCCTTGGTA-3′; and SP1–miR-218: Forward 5′-CTCGAGGATGTTTTCCCTTAACTTTTCCT-3′, Reverse 5′-TCT AGACTAAAAGCTTATATCCTCAGCATC-3′. Each of the forward and reverse primers carried the *XhoI* and *XbaI* sites at their 5′-ends. The obtained DNA fragments were inserted into the pmirGLO Vector (Promega, San Luis Obispo, CA, USA). The resulting vectors were dubbed pCol1A1–miR-29/mirGLO, pCol1A1–miR-143/mirGLO, pCol1A1–miR-218/mirGLO, pSP1–miR-29/mirGLO, and pSP1–miR-218/mirGLO. Human stellate cells were seeded on 96-well plates (Microtest 96-well Assay Plate; Becton Dickinson, Franklin Lakes, NJ, USA) in DMEM supplemented with 10% FBS at a density of 2 × 10^4 cells/well. The following day, they were transfected with 200 ng of reporter plasmid along with miRNA precursors using Lipofectamine 2000 as described above and incubated for an additional 24 h. After incubation, the medium was removed from the wells, and 20 μl of phosphate-buffered saline was added. The Dual-Glo Luciferase Assay System (Promega) was used to analyze luciferase expression according to the manufacturer's protocol. Firefly luciferase activity was normalized to *Renilla* luciferase activity to adjust for variations in transfection efficiency among experiments.

Statistical analysis. Data presented as bar graphs are the means ± SD of at least three independent experiments. Statistical analysis was performed using Student's *t*-test, and $P < 0.05$ was considered significant.

Results and discussion

Regulation of Col1A1 expression by TGF-β1 and IFNα in human stellate cells

Immortalized human stellate cells, LX-2, are classified as an activated phenotype that expresses mRNAs for Col1A1 and other fibrogenetic molecules and are reported to be highly gene-transfectable [24]. At first, we observed that Col1A1 mRNA expression increased dose-dependently by TGF-β1 (Fig. 1A), whereas this upregulation was significantly inhibited by the presence of 100 IU/ml of human IFNα (Fig. 1B).

Extraction of miR-29b, -143, and -218 as candidates interacting with Col1A1 3′UTR

To determine the role of miRNAs in human stellate cell collagen expression, we searched for predictable miRNAs that could interact

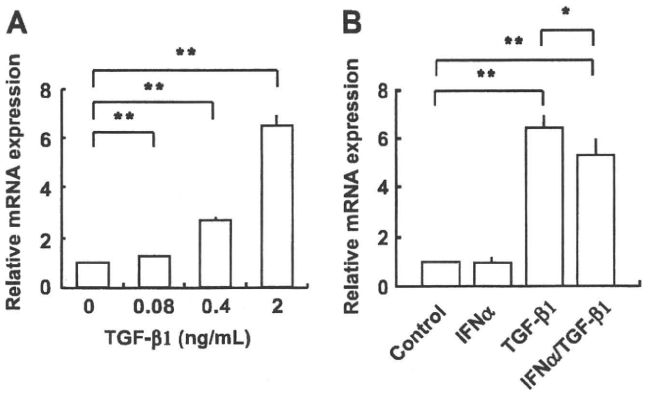

Fig. 1. Regulation of alpha 1 (I) collagen (Col1A1) expression in human stellate cells. (A) Dose-dependent effect of TGF-β1 on Col1A1 mRNA expression. Human stellate cells, LX-2, were treated with TGF-β1 (0, 0.08, 0.4, and 2 ng/ml) for 24 h in DMEM containing 0.1% FBS. (B) Effect of IFNα on Col1A1 mRNA expression in human stellate cells stimulated with TGF-β1. The cells were treated with IFNα (100 IU/ml), TGF-β1 (2 ng/ml), or IFNα (100 IU/ml) + TGF-β1 (2 ng/ml) for 24 h in DMEM containing 0.1% FBS. Control: human stellate cells were cultured for 24 h in DMEM containing 0.1% FBS. mRNA expression was analyzed by real-time PCR. The results are expressed as relative expression against control expression without treatment. $^{*}P < 0.05$; $^{**}P < 0.01$.

with 3′UTR of human Col1A1 mRNA using TargetScan Human Release 5.1 (http://www.targetscan.org/). As a result, miR-29, -98, -129, -133, -143, -196, -218, and let-7 were extracted as candidates. Because further *in silico* analyses among the eight candidates indicated that miR-29b, -143, and -218 were highly homologous to the Col1A1 3′UTR, we checked the expression levels of these miRNAs in human stellate cells by real-time PCR. As a result, miR-143 and -218 expressions were up and downregulated dose-dependently by TGF-β1, respectively, (Fig. 2A and B). Although miR-29b expression was unaffected by TGF-β1, it increased in

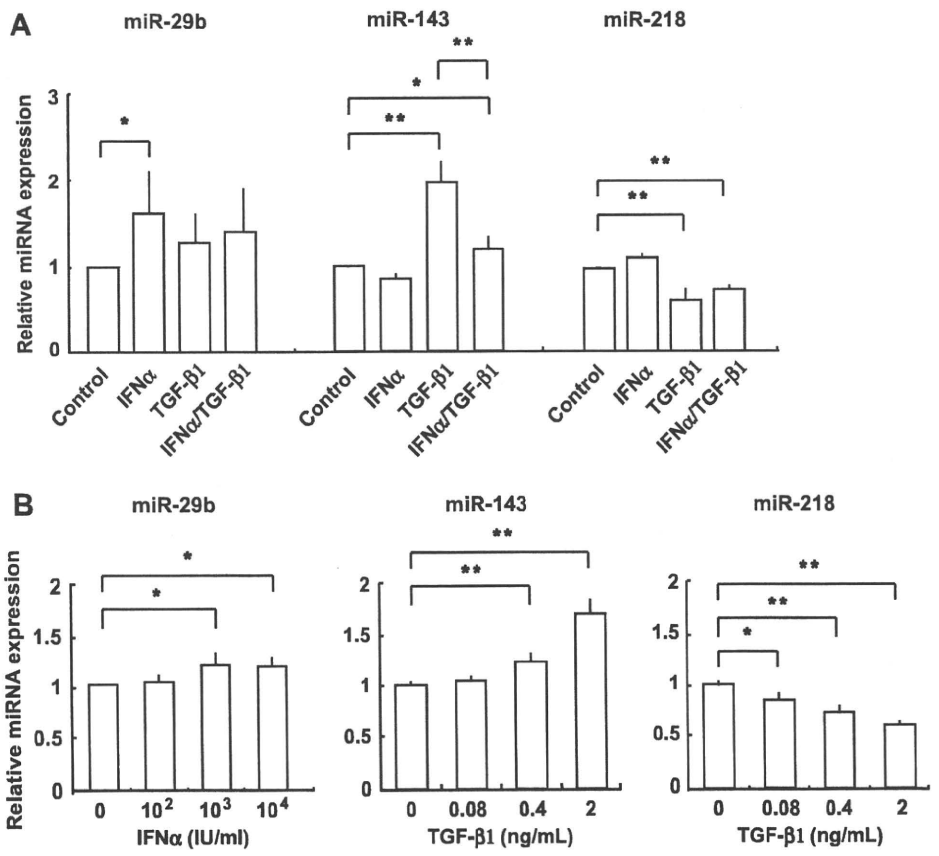

Fig. 2. Expression of miR-29b, -143, and -218 in human stellate cells. (A) Expression of miR-29b, -143, and -218 in human stellate cells, LX-2. The cells were treated with IFNα (100 IU/ml), TGF-β1 (2 ng/ml), or IFNα (100 IU/ml) + TGF-β1 (2 ng/ml) for 24 h in DMEM containing 0.1% FBS. Control: human stellate cells were cultured for 24 h in DMEM containing 0.1% FBS. (B) Dose-dependent effect of IFNα or TGF-β1 on the expression of miR-29b, -143, and -218 in human stellate cells. miRNA expression was analyzed by real-time PCR. The results are expressed as relative expression against control expression without treatment. $^{*}P < 0.05$; $^{**}P < 0.01$.

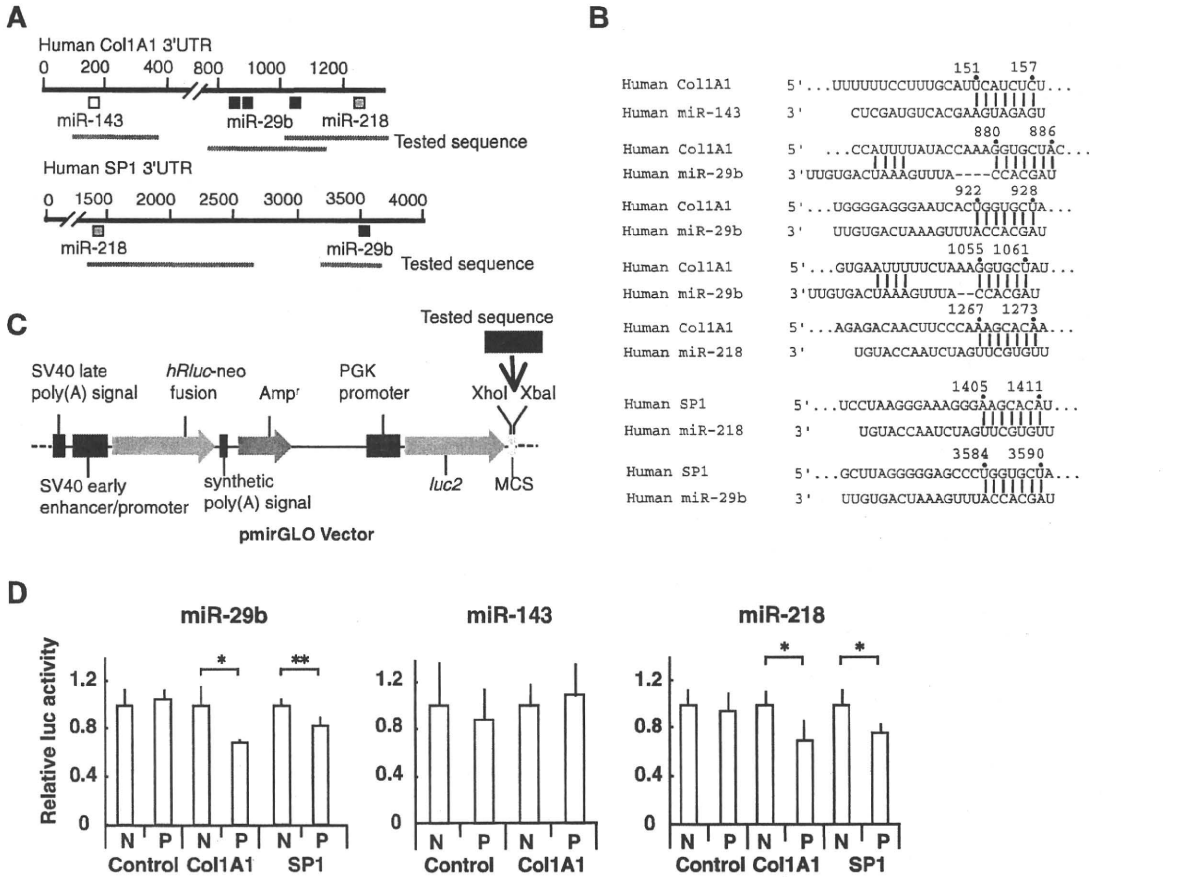

Fig. 3. Interaction of miR-29b, -143, and -218 with the 3′UTRs of alpha 1 (I) collagen (Col1A1) and SP1 mRNAs. (A) Schematic indication of the miRNA binding sites in the 3′UTRs of Col1A1 and SP1 mRNAs based on TargetScan Human Release 5.1 (http://www.targetscan.org/). Each black, white, and gray box indicates miR-29b, -143, and -218, respectively. Tested sequences indicate the regions that were inserted into the luciferase reporter vector. (B) Predicted consequential pairing of the target region and miRNAs. Arabic numerals above indicate the positions relative to the 3′UTR start sites. (C) Luciferase reporter vector structure. The vector contained two expression units; one for the *Renilla* luciferase gene (*hRluc*-neo fusion) expression. This unit was driven by an SV40 early promoter. The other was for the firefly luciferase gene (*luc2*). This unit was driven by a human phosphoglycerate kinase (PGK) promoter and contained multiple cloning sites (MCS) downstream of the *luc2* sequence. Each Col1A1 and SP1 3′UTR containing a putative miRNA target region (tested sequence) was cloned into the MCS. Arrows indicate the gene directions. Amp^R indicates an ampicillin-resistant plasmid gene. (D) Interaction of miR-29b, -143, and -218 with the 3′UTRs of Col1A1 and SP1 mRNAs in human stellate cells. Relative luciferase activity derived from pCol1A1–miR-29/mirGLO and pSP1–miR-29/mirGLO in the presence of miR-29b precursors (left panel), pCol1A1–miR-143/mirGLO in the presence of miR-143 precursors (center panel), and pCol1A1–miR-218/mirGLO and pSP1–miR-218/mirGLO in the presence of miR-218 precursors (right panel). The pmirGLO vector was used as a negative control reporter vector (control). N: cotransfection of reporter vectors along with negative control precursors, which have a scrambled sequence. P: cotransfection of reporter vectors along with miRNA precursors. Firefly and *Renilla* luciferase activities were determined, and firefly luciferase was normalized to *Renilla* luciferase activity. Results are expressed as relative activities against the activity in the presence of negative control precursors. $^{*}P < 0.05$ and $^{**}P < 0.01$.

the presence of IFNα (Fig. 2A and B). Thus, we assumed that these miRNAs might affect type I collagen expression via their interaction with Col1A1 3′UTR in human stellate cells.

Interaction of miR-29b, -143, and -218 with 3′UTRs of Col1A1 and SP1 mRNAs

The prediction of miRNA target regions on Col1A1 3′UTR by TargetScan indicated that Col1A1 3′UTR has three target regions for miR-29b, one for miR-143, and one for miR-218 (Fig. 3A and B). Because collagen gene expression is regulated by miR-192 via an interaction with the transcriptional repressor E-box [26], we additionally considered SP1, which is a transcriptional regulator of Col1A1 expression induced by TGF-β1 [27,28]. The predicted miRNA target regions of SP1 3′UTR contained one target region for miR-29b and one for miR-218 (Fig. 3A and B).

To investigate the direct targeting of Col1A1 by miR-29b, -143, and -218 and that of SP1 by miR-29b and -218, the sequence of each target region was cloned and inserted into the downstream region of the firefly luciferase reporter gene (Fig. 3C). The resulting vectors were dubbed pCol1A1–miR-29/mirGLO, pCol1A1–miR-143/mirGLO, pCol1A1–miR-218/mirGLO, pSP1–miR-29/mirGLO, and pSP1–miR-218/mirGLO. These vectors were cotransfected into human stellate cells with miRNA precursors. As a result, the miR-29b and -218 precursors inhibited luciferase activity derived from the vectors carrying Col1A1 or SP1 3′UTRs (Fig. 3D). In contrast, the miR-143 precursors had no effect on luciferase activity of the vector carrying Col1A1 3′UTR (Fig. 3D). According to these observations, we assumed that the Col1A1 and SP1 3′UTR sequences could be targeted by miR-29b and -218, whereas miR-143, which was induced by TGF-β1 (Fig. 2A and B), had a negligible effect on Col1A1 expression in human stellate cells.

Regulation of type I collagen expression by miR-29b and -218

Next, we examined the effect of miR-29b and -218 overexpression on type I collagen mRNA and protein expression in human stellate cells. Transient transfection of miR-29b precursors signifi-

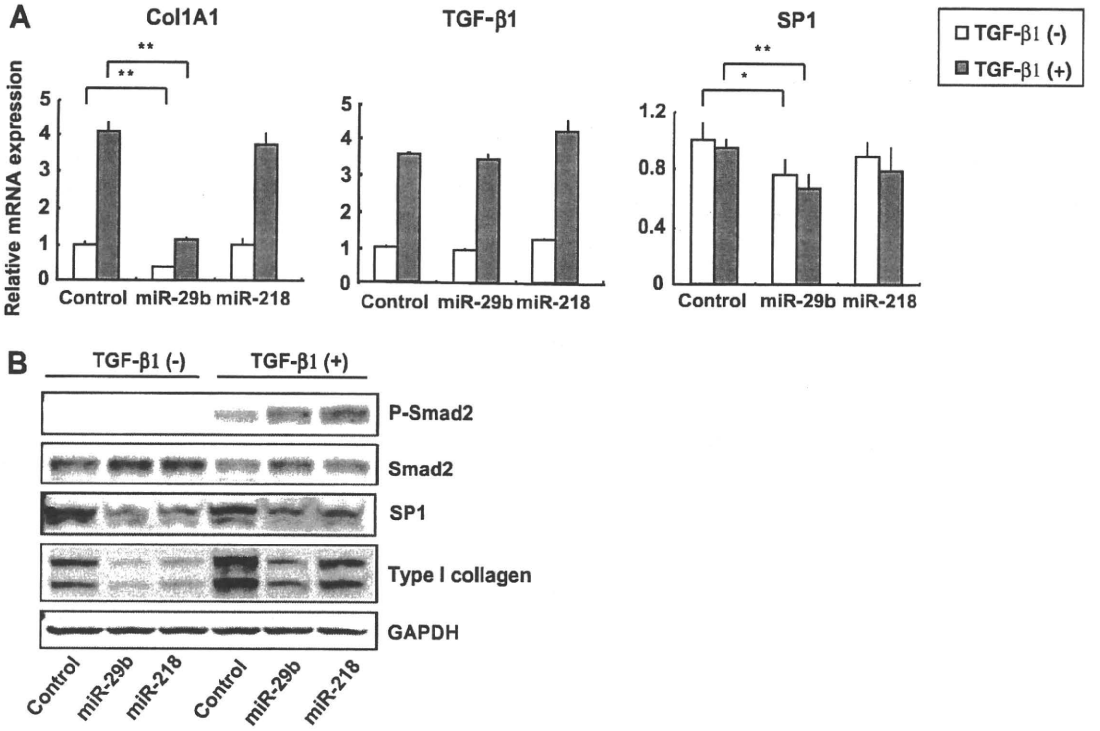

Fig. 4. Effect of miR-29b and -218 on type I collagen expression in human stellate cells. Human stellate cells were cultured in DMEM supplemented with 10% FBS and were transfected with 50 nM miR-29b, -218 precursors, or a negative control, which had a scrambled sequence (control) using Lipofectamine 2000. After 6 h, the medium was changed to DMEM containing 0.1% FBS with or without 2 ng/ml TGF-β1, and the culture was continued for another 24 h. (A) Effect of miR-29b and -218 precursors on the expression of Col1A1, TGF-β1, and SP1 mRNAs in human stellate cells with (gray column) or without (white column) TGF-β1. mRNA expression was analyzed by real-time PCR. The results are expressed as relative expression against control expression. $^{*}P < 0.05$; $^{**}P < 0.01$. (B) Effect of miR-29b and -218 precursors on the protein expression of phospho-Smad2 (P-Smad2), Smad2, SP1, type I collagen, and GAPDH in human stellate cells in the presence (+) or absence (−) of TGF-β1.

cantly inhibited type I collagen mRNA and protein expression (Fig. 4A, left panel, and B) in unstimulated human stellate cells. Additionally, transfection of miR-29b precursors completely suppressed the upregulation of type I collagen mRNA and protein under TGF-β1 stimulation. TGF-β1 stimulation induces Col1A1 mRNA expression through a pathway that includes SP1 and phosphorylated Smad2/3 [29]. In our results, upregulation of TGF-β1 mRNA (Fig. 4A, center panel) and phosphorylation of Smad2 (Fig. 4B) under TGF-β1 stimulation were unaffected by the transfection of miR-29b precursors. These results suggested that miR-29b may affect the downstream of phosphorylated Smad2. Moreover, the transfection of miR-29b precursors decreased SP1 mRNA and protein expression (Fig. 4A, right panel, and B). Thus, the miR-29b-induced repression of type I collagen expression could be caused by its direct interaction with Col1A1 3′UTR and additionally by its interaction with SP1 expression in human stellate cells. These observations agree with a report showing the role of miR-29 in collagen expression and cardiac fibrosis after cardiac infarction [30]. In contrast, transfection of miR-218 precursors triggered a negligible change in Col1A1 and SP1 mRNA expression (Fig. 4A, left and right panels) but slightly reduced their protein level (Fig. 4B). Taken together, these results imply that miR-29b is the most potent miRNA with regard to collagen production in human stellate cells.

Conclusions

We found a potent repression of collagen production by miR-29b in human stellate cells. IFNs attenuate and may regress liver fibrosis caused by hepatitis C viral infection [21–23], although the precise molecular mechanism has yet to be demonstrated. The present study using human stellate cells demonstrated that IFNα upregulates miR-29b (Fig. 2B and C), which is a negative regulator of type I collagen production via the interaction with Col1A1 and SP1 3′UTRs. This observation implies the contribution of miR-29b to antifibrotic IFN actions. Targeted delivery of miR-29b to activated stellate cells in the liver could become a new therapeutic strategy for human liver fibrosis in the future.

Acknowledgment

This work was supported by a grant from the Ministry of Health, Labour and Welfare of Japan to N. Kawada (2008–2009).

References

[1] R. Bataller, D.A. Brenner, Hepatic stellate cells as a target for the treatment of liver fibrosis, Semin. Liver Dis. 21 (2001) 437–451.
[2] S.L. Friedman, Molecular regulation of hepatic fibrosis, an integrated cellular response to tissue injury, J. Biol. Chem. 275 (2000) 2247–2250.
[3] N. Kawada, The hepatic perisinusoidal stellate cell, Histol. Histopathol. 12 (1997) 1069–1080.
[4] S. Dooley, B. Delvoux, B. Lahme, K. Mangasser-Stephan, A.M. Gressner, Modulation of transforming growth factor beta response and signaling during transdifferentiation of rat hepatic stellate cells to myofibroblasts, Hepatology 31 (2000) 1094–1106.
[5] E. Albanis, S.L. Friedman, Hepatic fibrosis. Pathogenesis and principles of therapy, Clin. Liver Dis. 5 (2001) 315–334. v–vi.
[6] W. Filipowicz, S.N. Bhattacharyya, N. Sonenberg, Mechanisms of post-transcriptional regulation by microRNAs: are the answers in sight?, Nat Rev. Genet. 9 (2008) 102–114.
[7] D.P. Bartel, MicroRNAs: genomics, biogenesis, mechanism, and function, Cell 116 (2004) 281–297.
[8] J. Brennecke, D.R. Hipfner, A. Stark, R.B. Russell, S.M. Cohen, Bantam encodes a developmentally regulated microRNA that controls cell proliferation and regulates the proapoptotic gene hid in *Drosophila*, Cell 113 (2003) 25–36.

[9] G.M. Schratt, F. Tuebing, E.A. Nigh, C.G. Kane, M.E. Sabatini, M. Kiebler, M.E. Greenberg, A brain-specific microRNA regulates dendritic spine development, Nature 439 (2006) 283–289.
[10] C.Z. Chen, L. Li, H.F. Lodish, D.P. Bartel, MicroRNAs modulate hematopoietic lineage differentiation, Science 303 (2004) 83–86.
[11] J. Kota, R.R. Chivukula, K.A. O'Donnell, E.A. Wentzel, C.L. Montgomery, H.W. Hwang, T.C. Chang, P. Vivekanandan, M. Torbenson, K.R. Clark, J.R. Mendell, J.T. Mendell, Therapeutic microRNA delivery suppresses tumorigenesis in a murine liver cancer model, Cell 137 (2009) 1005–1017.
[12] J.F. Chen, E.P. Murchison, R. Tang, T.E. Callis, M. Tatsuguchi, Z. Deng, M. Rojas, S.M. Hammond, M.D. Schneider, C.H. Selzman, G. Meissner, C. Patterson, G.J. Hannon, D.Z. Wang, Targeted deletion of Dicer in the heart leads to dilated cardiomyopathy and heart failure, Proc. Natl. Acad. Sci. USA 105 (2008) 2111–2116.
[13] D.O. Perkins, C.D. Jeffries, L.F. Jarskog, J.M. Thomson, K. Woods, M.A. Newman, J.S. Parker, J. Jin, S.M. Hammond, MicroRNA expression in the prefrontal cortex of individuals with schizophrenia and schizoaffective disorder, Genome Biol. 8 (2007) R27.
[14] I.M. Pedersen, G. Cheng, S. Wieland, S. Volinia, C.M. Croce, F.V. Chisari, M. David, Interferon modulation of cellular microRNAs as an antiviral mechanism, Nature 449 (2007) 919–922.
[15] J. Ji, J. Shi, A. Budhu, Z. Yu, M. Forgues, S. Roessler, S. Ambs, Y. Chen, P.S. Meltzer, C.M. Croce, L.X. Qin, K. Man, C.M. Lo, J. Lee, I.O. Ng, J. Fan, Z.Y. Tang, H.C. Sun, X.W. Wang, MicroRNA expression, survival, and response to interferon in liver cancer, N. Engl. J. Med. 361 (2009) 1437–1447.
[16] C.E. Rogler, L. Levoci, T. Ader, A. Massimi, T. Tchaikovskaya, R. Norel, L.E. Rogler, MicroRNA-23b cluster microRNAs regulate transforming growth factor-beta/bone morphogenetic protein signaling and liver stem cell differentiation by targeting Smads, Hepatology 50 (2009) 575–584.
[17] C. Esau, S. Davis, S.F. Murray, X.X. Yu, S.K. Pandey, M. Pear, L. Watts, S.L. Booten, M. Graham, R. McKay, A. Subramaniam, S. Propp, B.A. Lollo, S. Freier, C.F. Bennett, S. Bhanot, B.P. Monia, MiR-122 regulation of lipid metabolism revealed by in vivo antisense targeting, Cell Metab. 3 (2006) 87–98.
[18] L. Zheng, G.C. Lv, J. Sheng, Y.D. Yang, Effect of miRNA-10b in regulating cellular steatosis level by targeting PPAR-alpha expression, a novel mechanism for the pathogenesis of NAFLD, J. Gastroenterol. Hepatol. (2009).
[19] J. Ji, J. Zhang, G. Huang, J. Qian, X. Wang, S. Mei, Over-expressed microRNA-27a and 27b influence fat accumulation and cell proliferation during rat hepatic stellate cell activation, FEBS Lett. 583 (2009) 759–766.
[20] C.J. Guo, Q. Pan, D.G. Li, H. Sun, B.W. Liu, MiR-15b and miR-16 are implicated in activation of the rat hepatic stellate cell: an essential role for apoptosis, J. Hepatol. 50 (2009) 766–778.
[21] Y. Shiratori, F. Imazeki, M. Moriyama, M. Yano, Y. Arakawa, O. Yokosuka, T. Kuroki, S. Nishiguchi, M. Sata, G. Yamada, S. Fujiyama, H. Yoshida, M. Omata, Histologic improvement of fibrosis in patients with hepatitis C who have sustained response to interferon therapy, Ann. Intern. Med. 132 (2000) 517–524.
[22] T. Poynard, J. McHutchison, G.L. Davis, R. Esteban-Mur, Z. Goodman, P. Bedossa, J. Albrecht, Impact of interferon alfa-2b and ribavirin on progression of liver fibrosis in patients with chronic hepatitis C, Hepatology 32 (2000) 1131–1137.
[23] Y. Inagaki, T. Nemoto, M. Kushida, Y. Sheng, K. Higashi, K. Ikeda, N. Kawada, F. Shirasaki, K. Takehara, K. Sugiyama, M. Fujii, H. Yamauchi, A. Nakao, B. De Crombrugghe, T. Watanabe, I. Okazaki, Interferon alfa down-regulates collagen gene transcription and suppresses experimental hepatic fibrosis in mice, Hepatology 38 (2003) 890–899.
[24] L. Xu, A.Y. Hui, E. Albanis, M.J. Arthur, S.M. O'Byrne, W.S. Blaner, P. Mukherjee, S.L. Friedman, F.J. Eng, Human hepatic stellate cell lines, LX-1 and LX-2: new tools for analysis of hepatic fibrosis, Gut 54 (2005) 142–151.
[25] K. Otogawa, T. Ogawa, R. Shiga, K. Nakatani, K. Ikeda, Y. Nakajima, N. Kawada, Attenuation of acute and chronic liver injury in rats by iron-deficient diet, Am. J. Physiol. Regul. Integr. Comp. Physiol. 294 (2008) R311–R320.
[26] M. Kato, J. Zhang, M. Wang, L. Lanting, H. Yuan, J.J. Rossi, R. Natarajan, MicroRNA-192 in diabetic kidney glomeruli and its function in TGF-beta-induced collagen expression via inhibition of E-box repressors, Proc. Natl. Acad. Sci. USA 104 (2007) 3432–3437.
[27] L. Li, C.M. Artlett, S.A. Jimenez, D.J. Hall, J. Varga, Positive regulation of human alpha 1 (I) collagen promoter activity by transcription factor Sp1, Gene 164 (1995) 229–234.
[28] I. Garcia-Ruiz, P. de la Torre, T. Diaz, E. Esteban, I. Fernandez, T. Munoz-Yague, J.A. Solis-Herruzo, Sp1 and Sp3 transcription factors mediate malondialdehyde-induced collagen alpha 1 (I) gene expression in cultured hepatic stellate cells, J. Biol. Chem. 277 (2002) 30551–30558.
[29] P. Sysa, J.J. Potter, X. Liu, E. Mezey, Transforming growth factor-beta1 up-regulation of human alpha(1) (I) collagen is mediated by Sp1 and Smad2 transacting factors, DNA Cell Biol. 28 (2009) 425–434.
[30] E. van Rooij, L.B. Sutherland, J.E. Thatcher, J.M. DiMaio, R.H. Naseem, W.S. Marshall, J.A. Hill, E.N. Olson, Dysregulation of microRNAs after myocardial infarction reveals a role of miR-29 in cardiac fibrosis, Proc. Natl. Acad. Sci. USA 105 (2008) 13027–13032.

Journal of Viral Hepatitis, 2010, **17**, 123–129 doi:10.1111/j.1365-2893.2009.01160.x

Add-on combination therapy with adefovir dipivoxil induces renal impairment in patients with lamivudine-refractory hepatitis B virus

A. Tamori,[1] M. Enomoto,[1] S. Kobayashi,[1] S. Iwai,[1] H. Morikawa,[1] H. Sakaguchi,[1] D. Habu,[2] S. Shiomi,[3] Y. Imanishi[4] and N. Kawada[1] [1]*Department of Hepatology, Osaka City University Graduate School of Medicine, Osaka, Japan;* [2]*Department of Medical Nutrition, Osaka City University Graduate School of Life Science, Osaka, Japan;* [3]*Department of Nuclear Medicine, Osaka City University Graduate School of Medicine, Osaka, Japan; and* [4]*Department of Metabolism, Endocrinology and Molecular Medicine, Osaka City University Graduate School of Medicine, Osaka, Japan*

Received January 2009; accepted for publication March 2009

SUMMARY. Combination therapy with adefovir dipivoxil (ADV) and lamivudine (LAM) is recommended for patients infected with LAM-refractory hepatitis B virus (HBV). However, the effects of such therapy on renal function and serum phosphorus levels have not been fully evaluated. Combination therapy with ADV and LAM was given to 37 patients infected with LAM-refractory HBV, including 17 with hepatic cirrhosis. Serum HBV DNA levels decreased to below 2.6 $\log_{10}$ copies/mL in 23 (62%) of 37 patients at 12 months, 25 (78%) of 32 patients at 24 months, and 16 (84%) of 19 patients at 36 months. Except for one cirrhotic patient, serum alanine aminotransferase levels were below 50 IU/L in all patients during combination therapy. Serum creatinine levels increased in 14 (38%) of 37 patients, and serum phosphate levels decreased to below 2.5 mg/mL in 6 (16%) of 37 patients during combination therapy. Patients who received combination therapy for 36 months or longer had a significantly incidence of elevated serum creatinine levels. Fanconi syndrome occurred in a 57-year-old woman with cirrhosis after ADV was added to LAM. Combination therapy with ADV and LAM can maintain biochemical remission in patients with LAM-refractory HBV. However, the dosing interval of ADV should be adjusted according to renal function and serum phosphate levels in patients receiving long-term treatment.

Keywords: adefovir dipivoxil, Fanconi syndrome, hepatitis B virus, lamivudine.

INTRODUCTION

Hepatitis B virus (HBV) is a widely prevalent pathogen that causes chronic hepatitis, hepatic cirrhosis, and hepatocellular carcinoma (HCC) [1]. Interferon and nucleos(t)ide analogues are used for antiviral therapy in patients infected with chronic hepatitis B infection [2,3]. Lamivudine (LAM) is the first nucleoside analogue approved for the treatment of HBV-infected liver disease. LAM suppresses HBV replication in most patients and improves hepatic inflammation [4]. However, more than 60% of patients with HBV who receive long-term LAM therapy become resistant to the drug within 4 years after starting treatment [5]. For LAM-resistant HBV, a switching-to adefovir dipivoxil (ADV) or entecavir (ETV) treatment is a choice of treatment [6,7]. However, in ADV monotherapy for LAM-refractory chronic hepatitis B, virological breakthrough due to development of ADV resistant mutations occurred in three (21%) of 14 patients within 18 months [8]. In another study, ETV-resistant mutations developed in 12 (8%) of 151 patients with LAM-refractory chronic hepatitis B who received 1 mg ETV once daily for 2 years [7]. In contrast, combination therapy with ADV and LAM decreased HBV DNA levels in patients with LAM-resistant HBV and maintained the effect without virological and biochemical breakthroughs for 3 years [8,9]. In one study performed in Japan, ADV-resistant mutations occurred in only 2 of 129 patients with LAM-refractory chronic hepatitis B who received ADV plus LAM for 2 years [10].

Abbreviations: AD, adefovir dipivoxil; ALT, alanine aminotransferase; anti-HBe, antibodies to HBeAg; ETV, entecavir; HBeAg, hepatitis B e antigen; HBsAg, hepatitis B surface antigen; HBV, hepatitis B virus; HCC, hepatocellular carcinoma; HIV, human immunodeficiency virus; LAM, lamivudine; TDF, tenofovir disoproxil fumarate.

Correspondence: Akihiro Tamori, MD, Department of Hepatology, Osaka City University Graduate School of Medicine, 1-4-3 Asahimachi, Abeno-ku, Osaka 545-8585, Japan. E-mail: atamori@med.osaka-cu.ac.jp

These studies concluded that combination therapy with ADV and LAM was the treatment of choice for patients with LAM-resistant HBV.

An important limitation of previous studies of combination therapy with ADV and LAM is the lack of adequate safety data. Monotherapy with LAM is given to more than 30 000 patients with HBV-related chronic liver disease in Japan. LAM has not been reported to induce serious adverse effects, except for the emergence of LAM-resistant HBV. On the other hand, nephrotoxicity is the dose-limiting adverse effect in the use of ADV. In phase III, randomized, controlled studies, there were no increases from baseline of 0.5 mg/dL or greater in the serum creatinine level and no confirmed instances of serum phosphate levels below 2.0 mg/dL during 48 weeks of monotherapy with 10 mg ADV [11]. However, the renal safeness of combination therapy with ADV and LAM in long-term use is not enough to be evaluated. In particular, there are few reports about decrease of serum phosphate during the combination therapy. In our hospital, an open-label study of long-term add-on treatment with ADV in patients with LAM-refractory HBV has been in progress since 2003.

In the present study, we investigated the incidence of serum creatinine increase and hypophosphorus in patients with HBV-related chronic liver diseases during long-term ADV and LAM combination therapy. In addition, clinical characteristics of patients in whom mild renal impairment was observed were evaluated, since early detection of adverse event is important.

METHODS

Patients

The study group comprised 37 consecutive Japanese patients with LAM-refractory HBV who received a combination of 100 mg of LAM plus 10 mg of ADV daily for more than 1 year in Osaka City University Hospital between September 2002 and November 2008 (Table 1). All patients had a 1.5-$\log_{10}$ copies/mL or greater increase in the serum HBV DNA level during LAM treatment. No patient had a history of treatment with other nucleoside analogues, such as ETV and famciclovir. Patients were excluded if they had antibodies to hepatitis C virus or human immunodeficiency virus (HIV). Serum creatinine levels were under 1.2 mg/dL in all patients, and creatinine clearance was over 50 mL/min in all patients except one, who had a value of 45.5 mL/min. Before adding ADV to LAM, 10 patients received curative treatment for HCC. Liver biopsy was performed in 25 patients. Hepatic cirrhosis was histologically diagnosed in 13 patients and clinically diagnosed in 4 patients with oesophageal varices. All patients gave written informed consent to undergo viral sequencing and to participate in this study.

Analysis of serological markers for HBV

Hepatitis B surface antigen (HBsAg), hepatitis B e antigen (HBeAg), and antibodies to HBeAg (anti-HBe) in patient sera were tested by enzyme immunoassay, radioimmunoassay, or both, using commercially available kits (Dainabott, Tokyo, Japan).

Analysis of DNA markers for HBV

Genotypes of HBV were identified by enzyme-linked immunosorbent assay with monoclonal antibodies to type-specific epitopes in the preS2-region (Institute of Immunology, Tokyo, Japan), as described elsewhere [12]. HBV DNA was measured by transcription-mediated amplification (TMA) with a hybridization protection assay (Chugai Diagnostics, Tokyo, Japan) [13]. The detection range of the TMA assay was between 3.7 and 8.7 $\log_{10}$ copies/mL of HBV DNA. If HBV DNA was not detected by this method, we tried again, using the polymerase chain reaction (PCR)-based Amplicor Monitor test (Roche Diagnostics, Tokyo, Japan) [14]. The detection range of the PCR assay was between 2.6 and 7.6

Table 1 Patients' characteristics at the start of adding adefovir to lamivudine

Average age years (min–max)	55 (33–69)
Gender (male/female)	25/12
Prior LAM therapy duration (min–max)	30 months (8–64)
ADV treatment duration (min–max)	38 months (15–68)
Presence of cirrhosis	17
Past history of HCC treatment	10
HBV genotype: A, B, C	2, 1, 34
HBeAg positive/negative	25/12
HBV DNA Log/mL (min–max)	6.6 (4.2–8.6)
ALT IU/L (min–max)	149 (30–397)
Histological examination (F1, F2, F3, F4, not done)	(6, 6, 0, 13, 12)
Phosphate mg/dL (min–max)	3.4 (2.6–4.6)
Creatinine mg/dL (min–max)	0.79 (0.52–1.1)
Creatinine clearance in mL/min (min–max)	87.4 (45.5–136.2)

$\log_{10}$ copies/mL. From 1 March 2008, HBV DNA was measured by the Taqman HBV test (Roche Diagnostics, Tokyo, Japan). The detection range of the Taqman HBV test is between 1.8 and 8.8 $\log_{10}$ copies/mL of HBV DNA [15].

LAM-resistant mutations in the tyrosine–methionine–aspartate–aspartate motif of the HBV polymerase gene, L80I, and ADV-resistant mutations were examined by a line-probe assay (INNO-LiPA HBV DR, Innogenetics NV, Belgium) [16].

Chemical markers in serum

Levels of alanine aminotransferase (ALT), creatinine, and phosphate were examined before and after combination therapy with ADV and LAM. Creatinine clearance was calculated with Cockcroft's formula before add-on treatment with ADV [17]. An increase in the serum creatinine level was defined as an increase equivalent to more than 130% of the creatinine level at the start of ADV add-on therapy, with no decrease in the absence of additional treatment.

Statistical analysis

Statistical analysis was performed with the Statview SE+Graphics program, version 5.0 (SAS Institute, Cary, NC, USA). The Mann–Whitney *U*-test was used to compare two continuous variables, and the chi-square test was used to compare two categorical variables. All tests were two-sided, and P values of <0.05 were considered to indicate statistical significance.

Ethical considerations

The study protocol complied with the ethical guidelines of the Declaration of Helsinki (1975) and was approved by the Ethics Committee of Osaka City University Graduate School of Medicine.

RESULTS

Baseline characteristics of patients with LAM-refractory HBV

The HBV genotype was A in 2 patients, B in 1, and C in 34 (Table 1). At the start of add-on treatment with ADV, HBeAg was positive in 25 of the 37 patients. On analysis of the LAM resistant motif, M204I mutations were detected in 12 patients, and M204V mutations were detected in 12. In 11 patients, both mutated motifs of HBV were detected. In one of the patients with both mutations, an additional mutation (L80I) was found. LAM-resistant motifs were not examined in the other two patients. ADV-resistant mutations (A181V/T or N236T) were not detected before the start of ADV add-on treatment in any patient with LAM-resistant HBV.

Virological response to combination therapy

HBV DNA decreased to below 2.6 $\log_{10}$ copies/mL in 23 (62%) of 37 patients with LAM-refractory HBV at 12 months, 25 (78%) of 32 patients at 24 months, 16 (84%) of 19 patients at 36 months, and 8 (80%) of 10 patients at 48 months (Fig. 1). In three patients with HBeAg, the HBV DNA level did not decrease to below 4 $\log_{10}$ copies/mL during more than 30 months of combination therapy. In two of these patients, who did not have cirrhosis, A181T mutations were detected 18 months after the start of ADV add-on therapy. A181V/T or N236T mutation was not detected in the other patient, who had cirrhosis and genotype C (Table 2). Combination therapy reduced the HBV DNA level to below 2.6 $\log_{10}$ copies/mL in 10 (59%) of 17 patients with hepatic cirrhosis at 12 months, and in 12 (80%) of 15 patients with hepatic cirrhosis at 24 months. Among the 10 patients who received curative treatment for HCC before add-on treatment with ADV, combination therapy reduced the HBV DNA level to below 2.6 $\log_{10}$ copies/mL in 6 (60%) of 10 patients at 12 months and 5 (83%) of 6 patients at 24 months.

Biochemical and serological responses to combination therapy

Serum ALT levels decreased to below 50 IU/L in 26 (70%) of 37 patients with LAM-resistant HBV at 6 months, 27 (73%) of 37 patients at 12 months, 26 (81.2%) of 32 patients at 24 months, 17 (89.4%) of 19 patients at 36 months, and 9 (90%) of 10 patients at 48 months. Except for one patient with hepatic cirrhosis, serum ALT levels fell to below 50 IU/L in all patients who received ADV and LAM combination therapy (Fig. 1). HBeAg became undetectable in 6 (24%) of 25 patients at 12 months, 10 (48%) of 21 patients at 24 months, and 5 (38%) of 13 patients at 36 months.

Incidence of HCC

In 2 of 10 cirrhotic patients who received curative treatment for HCC, secondary HCC appeared during combination therapy with ADV and LAM (Table 2). One patient with HCC recurrence continuously had a serum HBV DNA level of more than 4 $\log_{10}$ copies/mL. In 4 (14.8%) of 27 patients with LAM-refractory HBV, primary HCC appeared after adding ADV to LAM treatment. Two of the four patients in whom primary HCC developed had hepatic cirrhosis at the start of add-on treatment with ADV. In one patient with cirrhosis, the serum HBV DNA level exceeded 4 $\log_{10}$ copies/mL at the time of diagnosis of HCC. In the other three patients, serum HBV DNA levels remained below 2.6 $\log_{10}$ copies/mL on the occurrence of HCC. One patient died of advanced HCC 33 months after the start of combination therapy with ADV and LAM.

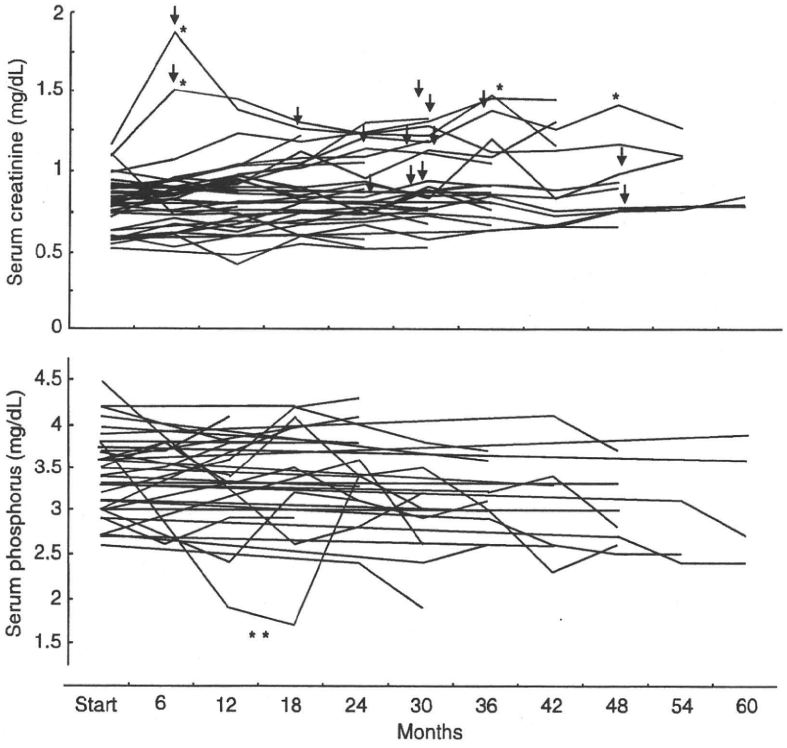

Fig. 1 Clinical courses after adding ADV to LAM in 37 patients with LAM-refractory HBV. In two patients with cirrhosis and two without cirrhosis whose serum creatinine levels rose to higher than 1.4 mg/dL, treatment with ADV was reduced from daily to every 2 days. Subsequently, the serum creatinine level decreased without reactivation of HBV replication. *Arrow* shows the time of an increase equivalent to more than 130% of the creatinine level at the start of ADV add-on therapy. *The times of adjusting the dose of ADV in the four patients with increased serum creatinine levels. **The time of adjusting the dose of ADV in a patient with Fanconi syndrome.

Table 2 Comparison of clinical characteristics and events between the cirrhotic and non-cirrhotic group during combination therapy

	Cirrhotic group	Non-cirrhotic group	*P*-value
n	17	20	
Average age years (min–max)	57 (47–69)	53 (33–68)	0.16
Gender (male/female)	13/4	10/7	0.48
Prior LAM therapy duration (min–max)	25 months (8–48)	34 months (11–64)	0.09
ADV treatment duration (min–max)	41 months (19–68)	36 months (15–65)	0.25
Past history of HCC treatment	8	2	0.03
HBeAg positive/negative	11/6	14/6	0.99
HBV DNA Log/mL (min–max)	6.4 (4.2–8.3)	6.9 (4.2–8.6)	0.28
Phosphate mg/dL (min–max)	3.3 (2.7–4.6)	3.4 (2.7–4.2)	0.61
Creatinine mg/dL (min–max)	0.78 (0.56–1.1)	0.82 (0.52–1.1)	0.42
Creatinine clearance mL/min (min–max)	85.9 (45.5–130.1)	86.4 (53.6–136.2)	0.95
Emergence of ADV-resistant HBV after adding ADV	1	2	0.88
Incidence of HCC (primary/secondary) after adding ADV	5 (2/3)	2 (2/0)	0.28

Renal impairment and hypophosphataemia during combination therapy

Serum creatinine levels gradually increased after the start of add-on treatment with 10 mg of ADV in 14 (38%) of 37 patients. In patients who received combination therapy for longer than 36 months or longer, the incidence of elevated serum creatinine levels increased significantly (Table 3). Serum creatinine did not increase in three patients whose HBV DNA level remained above 4 $\log_{10}$ copies/mL during more than 30 months of combination therapy. Except for these patients, there were no differences in clinical course between patients with creatinine increase and patients without it. In four patients (11%) whose serum creatinine levels increased to above 1.4 mg/dL, the dosing interval of ADV was adjusted to every 2 days. After this adjustment, serum creatinine levels decreased without reactivation of HBV replication. Two of these patients had progression to

Table 3 Comparison of clinical characteristics between patients with and those without an increase in serum creatinine levels

	Presence of creatinine increase	Absence of creatinine increase	*P*-value
N	14	23	
Average age years	59	53	0.07
Gender (male/female)	10/4	15/8	0.98
ADV treatment duration	45 months	34 months	0.02
Presence of cirrhosis (+/−)	9/5	8/15	0.16
HBV genotype: A, B, C	1, 0, 13	1, 1, 21	0.65
HBeAg positive/negative	11/3	14/9	0.45
HBV DNA Log/mL (min–max)	7	6.4	0.22
ALT (IU/L)	173	129	0.26
Creatinine (mg/dL)	0.82	0.77	0.35
Creatinine clearance (mL/min)	80.6	91.6	0.19

hepatic cirrhosis at the beginning of add-on treatment with ADV. The other patient without cirrhosis had hypertension as a complication. Creatinine clearance in this patient had decreased to 53.6 min/mL at the beginning of add-on treatment with ADV. The left patient did not have other complications.

Serum phosphate levels decreased to below 2.5 mg/mL in 6 (16%) of 37 patients. Serum creatinine levels increased in all six of these patients. No other variables correlated with decreased serum phosphate levels.

Case presentation

In December 2005, ADV was added to LAM therapy in a 57-year-old woman infected with YIDD-mutated HBV. She was given a clinical diagnosis of hepatic cirrhosis with no other complications, including HCC. Before combination therapy, HBeAg was negative, and the HBV DNA level was 6.5 $\log_{10}$ copies/mL. Creatinine and phosphate levels in serum were 0.56 and 3.8 mg/dL, respectively. The creatinine clearance was 56.7 mL/min. Nine months after starting combination therapy, severe lumbago developed. At 14 months, oedema of the legs and joint pain of the feet occurred. The serum alkaline phosphatase level increased to 800 IU/L, and she was admitted to our hospital. The serum HBV DNA level had decreased to less than 2.6 $\log_{10}$ copies/mL (Fig. 2). The serum phosphate level had decreased to 1.9 mg/dL, and the serum creatinine level was 0.88 mg/dL. Bone scintigraphy showed multiple-hot spots (Fig. 3). Urinalysis revealed glucosuria, proteinuria and generalized aminoaciduria. In

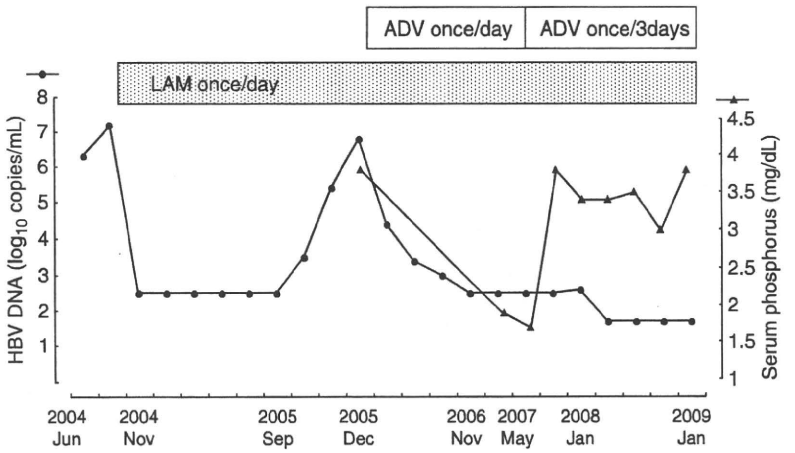

Fig. 2 Clinical course of a cirrhotic patient in whom Fanconi syndrome was induced by combination therapy. LAM treatment for HBV was started in November 2004. After 11 months, HBV DNA gradually increased, and LAM resistant YIDD-mutation was detected. In December 2005, 100 mg of ADV per day was added to LAM therapy. In May 2007, the HBV DNA level had decreased to less than 2.6 $\log_{10}$ copies/mL. However, the serum phosphate level fell to 1.9 mg/dL. After the dosing interval of ADV was adjusted to once every 3 days, the serum phosphate level increased to the normal range. The serum HBV DNA level has remained below 1.7 $\log_{10}$ copies/mL.

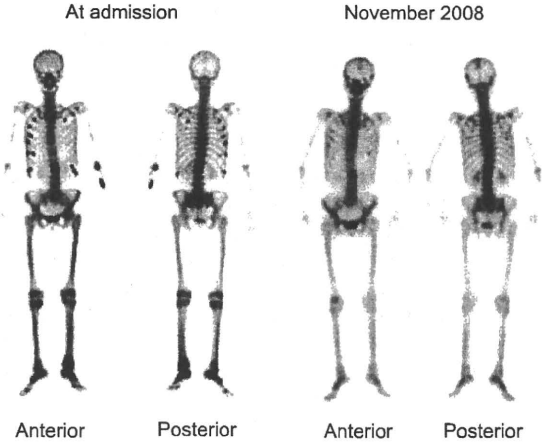

Fig. 3 Bone scintigrams of the patient in whom Fanconi syndrome was induced by combination therapy. At admission, there were many abnormal hot spots in the ribs, spine, sacrum, left humerus, and both legs. After reducing the dose of ADV and replenishment of phosphate, the abnormal spots disappeared except for the spine, which showed a compression fracture.

addition, the serum fibroblast growth factor 23 level had decreased to 3 pg/mL (normal range, 10–50 pg/mL). On the basis of these results, the patient was given a clinical diagnosis of osteomalacia due to secondary (drug-induced) Fanconi syndrome. The dosing interval of ADV was adjusted to once every 3 days, with replenishment of phosphate. After 1 month, the serum phosphate level increased dramatically to the normal range. The serum HBV DNA level has been maintained below 1.7 $\log_{10}$ copies/mL for 12 months with a combination of LAM daily and ADV every 3 days. In November 2008, the abnormal spots in bone improved without the continuous replenishment of phosphate.

DISCUSSION

Our study showed that the addition of ADV to LAM therapy decreased serum HBV DNA levels and improved elevated ALT levels in patients with LAM-refractory HBV. Combination therapy with ADV and LAM continued to be effective for more than 3 years in 19 patients. In 2 (5%) of 37 patients with LAM-resistant HBV, ADV-resistant mutants (A181T) were detected 18 months after the start of combination therapy. The effects of ADV add-on therapy in the present study were consistent with the results of previous studies [9,10]. In particular, our data showed that the antiviral effects of combination therapy in patients with hepatic cirrhosis and those who received treatment for HCC were not inferior to the effect in patients with chronic hepatitis. Three patients have received ADV add-on combination therapy for more than 5 years without elevation of HBV DNA levels. The latest examinations showed that ALT has remained below 40 IU/mL in 36 patients, including three infected with AVD-resistant HBV, during combination therapy. Although the sample size was small, our results suggest that combination therapy suppressed LAM-refractory HBV DNA levels in patients with cirrhosis or HCC and consistently improved elevated ALT levels, even after the emergence of A181T mutants.

Renal impairment is one of the most important adverse effects of ADV. The dosing interval of ADV should therefore be adjusted according to the creatinine clearance of patients. However, guidelines for dosage adjustment in patients given ADV plus LAM are lacking. In the present study, we evaluated the safety of treatment with ADV 10 mg daily added to LAM. Creatinine clearance was above 50 mL/min in all except one patient. In four (11%) patients, including one with a low creatinine clearance, the serum creatinine level increased to more than 1.4 mg/dL. After the interval between doses of ADV was adjusted to every 2 days, serum creatinine levels improved, with no increase in HBV DNA levels. A long-term study safety and efficacy study of ADV monotherapy showed that the serum creatinine level increased by at least 0.5 mg/dL as compared with the baseline value in 5 (8%) of 65 patients at 240 months [18]. In previous studies of ADV plus LAM combination therapy, daily treatment with ADV was shifted to every 2 days in 4 (3%) of 132 patients or 10 (7%) of 145 patients because the serum creatinine level rose by more than 0.5 mg/dL [9,10]. To evaluate slight alterations in renal function, we defined elevation of the serum creatinine level as a 30% increase from the baseline value. Elevations of serum creatinine were detected in 14 (38%) patients. The incidence of elevated serum creatinine levels was significantly higher in patients who received ADV plus LAM combination therapy for 36 months or longer. These results suggested that patients who receive long-term combination therapy are at risk for renal impairment. In the present study, 19 of 37 patients, including 17 with cirrhosis and 2 without cirrhosis who had received treatment for HCC, had a high risk of HCC. Computed tomography with contrast medium was repeatedly performed to detect the onset or recurrence of HCC. In addition to ADV, contrast medium might have contributed to renal impairment.

Some drugs have been reported to induce renal proximal tubulopathy in association with decreased reabsorption of phosphate. Serum phosphate concentrations were not enough to be evaluated in patients given ADV and LAM combination therapy. In our study, the serum phosphate level decreased to below 2.5 mg/mL in 6 (16.2%) of 37 patients during combination therapy. Serum creatinine levels increased in all six of these patients. It was suggested that decreased phosphate levels were accompanied by increased creatinine levels. In particular, Fanconi syndrome developed in one patient in whom the serum phosphate level decreased to 1.9 mg/dL. To our knowledge, this is the first case of combination therapy-related Fanconi syndrome to be reported. Tenofovir disoproxil fumarate (TDF), an anti- HIV drug, was approved for the treatment of patients with HBV

in the United States [19,20]. This is an acyclic nucleotide analogue with a molecular structure related to that of ADV. Recent study showed that 300 mg of TDF treatment had superior antiviral effect to patients with chronic hepatitis B compared to 10 mg of ADV treatment. The serious clinical adverse event related to TDF did not occurred during 48 weeks of the administration [21].

However, Fanconi syndrome was reported to have developed in a 45-year-old cirrhotic woman coinfected with HIV and HCV during treatment with TDF [22]. To quantify the risk of Fanconi syndrome, renal proximal tubulopathy should be assessed in large numbers of patients with HBV during nucleotide therapy, including a combination of ADV and LAM.

In conclusion, our study showed that combination therapy with ADV and LAM effectively suppressed HBV replication and maintained biochemical remission in patients who have chronic liver disease associated with LAM-refractory HBV. However, it is important to closely monitor renal function and serum phosphate levels in patients with cirrhosis, as well as those who receive long-term antiviral therapy. Renal impairment improved without increased HBV replication after adjusting the dosing interval of ADV.

ACKNOWLEDGEMENTS

We thank the staffs in the hepatitis research and prevention centre for their assistance in data/sample collection.

CONFLICT OF INTEREST

None.

REFERENCES

1 Ganem D. Hepatitis B virus infection-natural history and clinical consequences. *N Engl J Med* 2004; 350: 1118–1129.
2 Lok AS, McMahon BJ. Chronic hepatitis B: update of recommendations. *Hepatology* 2004; 39: 857–861.
3 Dienstag JL. Hepatitis B virus infection. *N Engl J Med* 2008; 359: 1486–1500.
4 Lai CL. A one-year trial lamivudine for chronic hepatitis B. Asia Hepatitis Lamivudine Study Group. *N Engl J Med* 1998; 339: 61–68.
5 Chen CH. Comparison of clinical outcome between patients continuing and discontinuing lamivudine therapy after biochemical breakthrough of YMDD mutants. *J Hepatol* 2004; 41: 454–461.
6 Peters MG, Hann Hw H, Martin P *et al.* Adefovir dipivoxil alone or in combination with lamivudine in patients with lamivudine-resistant chronic hepatitis B. *Gastroenterology* 2004; 126: 91–101.
7 Tenney DJ, Levine SM, Rose RE *et al.* Clinical emergence of entecavir-resistant hepatitis B virus requires additional substitutions in virus already resistant to lamivudine. *Antimicrob Agents Chemother* 2004; 48: 3498–3507.
8 Rapti I, Dimou E, Mitsoula P, Hadziyannis SJ. Adding-on versus switching-to adefovir therapy in lamivudine-resistant HBeAg-negative chronic hepatitis B. *Hepatology* 2007; 45: 307–313.
9 Lampertico P, Viganò M, Manenti E, Iavarone M, Sablon E, Colombo M. Low resistance to adefovir combined with lamivudine: a 3-year study of 145 lamivudine-resistant hepatitis B patients. *Gastroenterology* 2007; 133: 1445–1451.
10 Yatsuji H, Suzuki F, Sezaki H *et al.* Low risk of adefovir resistance in lamivudine-resistant chronic hepatitis B patients treated with adefovir plus lamivudine combination therapy: two-year follow-up. *J Hepatol* 2008; 48: 923–931.
11 Izzedine H, Hulot JS, Launay-Vacher V *et al.* Adefovir Dipivoxil International 437 Study Group; Adefovir Dipivoxil International 438 Study Group. Renal safety of adefovir dipivoxil in patients with chronic hepatitis B: two double-blind, randomized, placebo-controlled studies. *Kidney Int* 2004; 66: 1153–1158.
12 Usuda S, Okamoto H, Tanaka T *et al.* Differentiation of hepatitis B virus genotypes D and E by ELISA using monoclonal antibodies to epitopes on the preS2-region product. *J Virol Methods* 1999; 80: 97–112.
13 Ide T, Kumashiro R, Toyoda N, Matsuyama K, Miura T, Sata M. Second generation amplicor-HCV monitor assay: clinical features and predictors of the response to interferon. *Hepatol Res* 2000; 18: 230–238.
14 Gerken G, Gomes J, Lampertico P *et al.* Clinical evaluation and applications of the Amplicor HBV Monitor test, a quantitative HBV DNA PCR assay. *J Virol Methods* 1998; 74: 155–165.
15 Chevaliez S, Bouvier-Alias M, Laperche S, Pawlotsky JM. Performance of the Cobas AmpliPrep/Cobas TaqMan real-time PCR assay for hepatitis B virus DNA quantification. *J Clin Microbiol* 2008; 46: 1716–1723.
16 Stuyver L, Van Geyt C, De Gendt S *et al.* Line probe assay for monitoring drug resistance in hepatitis B virus-infected patients during antiviral therapy. *J Clin Microbiol* 2000; 38: 702–707.
17 Chantrel F, Enache I, Bouiller M *et al.* Abysmal prognosis of patients with type 2 diabetes entering dialysis. *Nephrol Dial Transpl* 1999; 14: 129–136.
18 Marcellin P, Chang TT, Lim SG *et al.* Long-term efficacy and safety of adefovir dipivoxil for the treatment of hepatitis B e antigen-positive chronic hepatitis B. *Hepatology* 2008; 48: 750–758.
19 van Bömmel F, Zöllner B, Sarrazin C *et al.* Tenofovir for patients with lamivudine-resistant hepatitis B virus (HBV) infection and high HBV DNA level during adefovir therapy. *Hepatology* 2006; 44: 318–325.
20 Keeffe EB, Dieterich DT, Han SH *et al.* A treatment algorithm for the management of chronic hepatitis B virus infection in the United States: 2008 update. *Clin Gastroenterol Hepatol* 2008; 6: 1315–1341.
21 Marcellin P, Heathcote EJ, Buti M *et al.* Tenofovir disoproxil fumarate versus adefovir dipivoxil for chronic hepatitis B. *N Engl J Med* 2008; 359: 2442–2455.
22 Verhelst D, Monge M, Meynard JL *et al.* Fanconi syndrome and renal failure induced by tenofovir: a first case report. *Am J Kidney Dis* 2002; 40: 1331–1333.

Hepatol Int (2009) 3:378–383
DOI 10.1007/s12072-008-9113-y

ORIGINAL ARTICLE

Induction of tropomyosin during hepatic stellate cell activation and the progression of liver fibrosis

Kohji Otogawa · Tomohiro Ogawa · Ryoko Shiga · Kazuo Ikeda · Norifumi Kawada

Received: 13 August 2008 / Accepted: 30 October 2008 / Published online: 10 December 2008

Abstract The activation of hepatic stellate cells (HSCs) is a cue to initiate liver fibrosis. Activated stellate cells acquire contractile activity similar to pericytes and myofibroblasts in other organs by inducing the contractile machinery of cytoskeletons such as smooth muscle α-actin (α-SMA), a well-known marker of activated stellate cells, and actin-binding proteins. We further show herein the expression of tropomyosin in rat HSCs in the course of their activation during primary culture and liver tissue damaged by thioacetamide intoxication. In immunoblot analysis, tropomyosin became detectable in an early stage of the primary culture of rat stellate cells in a manner similar to the expression of α-SMA and platelet-derived growth factor receptor-β. Tropomyosin was found to be colocalized with α-SMA on fluorescent immunocytochemistry. At the liver tissue level, an increased expression of tropomyosin was observed by immunoblot analysis and immunohistochemistry along the septum of fibrosis, where α-SMA was enriched. These results strongly suggest that tropomyosin is a new marker of activated stellate cells and may serve as a useful diagnostic marker of liver fibrosis.

Keywords Actin · Cell contraction · Vitamin A · Liver injury · Liver sinusoid

K. Otogawa · T. Ogawa · N. Kawada (✉)
Department of Hepatology, Graduate School of Medicine, Osaka City University, 1-4-3, Asahimachi, Abeno, Osaka 545-8585, Japan
e-mail: kawadanori@med.osaka-cu.ac.jp

R. Shiga · K. Ikeda
Department of Anatomy, Graduate School of Medicine, Osaka City University, Osaka, Japan

Abbreviations

DMEM	Dulbecco's modified Eagle's medium
ECM	Extracellular matrix
GAPDH	Glyceraldehyde-3-phosphate dehydrogenase
HSC	Hepatic stellate cell
PBS	Phosphate-buffered saline
PCR	Polymerase chain reaction
PDGFR-β	Platelet-derived growth factor receptor-β
TAA	Thioacetamide
α-SMA	Smooth muscle-α actin

Introduction

Hepatic stellate cells (HSCs) play a key role in liver fibrogenesis regardless of the pathogenesis [1–4]. In response to local tissue damage and hepatocyte necrosis, HSCs undergo activation characterized by the proliferation, migration, contraction, secretion of several profibrogenic mediators such as cytokines, growth factors, chemokines, and tissue inhibitors of matrix metalloproteinases, and generation of extracellular matrix (ECM) materials such as type I collagen. HSC activation thus contributes to scar formation in chronically injured liver tissue.

One of the indicators of activated HSCs is smooth muscle α-actin (α-SMA), the actin isoform typical of smooth muscle cell differentiation [5–10]. Similar to the expression of γ-actin, α-SMA was first demonstrated in primary-cultured rat HSCs in the course of the culture-dependent HSC activation process [5]. α-SMA-positive HSCs are also seen along the fibrotic septum of chronically damaged livers of rodent models, in which ECM proteins such as type I collagen and fibronectin are dominantly produced and deposited [11, 12]. Furthermore, in the human liver, the augmented expression of α-SMA has been